CHAPTER B: SEDIMENTARY PETROLOGY, RESERVOIR QUALITY, AND PROVENANCE OF ALBIAN–CENOMANIAN NANUSHUK FORMATION SANDSTONE, NPRA TEST WELLS, UMIAT 18, AND MEASURED OUTCROP SECTIONS, CENTRAL NORTH SLOPE, ALASKA

Kenneth P. Helmold[1] and David L. LePain[2]

INTRODUCTION

Hydrocarbon discoveries announced between 2015 and 2018 that are associated with stratigraphic traps in the Nanushuk Formation on the North Slope of Alaska have spurred renewed interest in exploration of the Colville basin. These discoveries form two roughly parallel fairways: a western trend that includes the Willow and West Willow oil accumulations and an eastern trend comprising the Pikka, Narwhal, and Horseshoe oil accumulations (fig. 1). Recoverable resources are estimated to be more than 300 million barrels at Willow and West Willow, and 500 to 1200 million barrels at Pikka, Narwhal, and Horseshoe (Houseknecht, 2019).

Exploration drilling in the area dates back nearly three quarters of a century to the U.S. Navy's Pet-4 exploration program that was conducted from 1944 to 1953 in the Naval Petroleum Reserve No. 4, currently known as the National Petroleum Reserve-Alaska (NPRA; Robinson and Collins, 1959). The Pet-4 program included detailed geologic field mapping that led to the documentation of numerous oil seeps. As part of this program, 45 shallow core tests and 36 shallow test wells were drilled to evaluate the petroleum potential of Cretaceous strata in the area (Gryc, 1988). Among the early wells are the U.S. Navy Fish Creek test well 1 (spudded May 17, 1949), U.S. Navy Square Lake test well 1 (spudded January 26, 1952), U.S. Navy Grandstand test well 1 (spudded May 1, 1952), and U.S. Navy Wolf Creek test well 3 (spudded August 20, 1952)—for simplicity, these wells will hereafter be referred to as Fish Creek 1, Square Lake 1, Grandstand 1, and Wolf Creek 3. Grandstand 1 is located outside of NPRA to the southeast but was drilled as part of the Pet-4 program and is considered an NPRA well for this report. The four wells were drilled by Arctic Contractors under contract to the U.S. Navy. Square Lake 1, Grandstand 1, and Wolf Creek 3 were drilled on anticlines (Robinson, 1958; Collins, 1959), whereas Fish Creek 1 was drilled near a surface oil seep (Robinson and Collins, 1959). The presence of oil seeps also led the Navy to drill eleven wells on a shallow faulted anticlinal structure in the southeastern portion of NPRA which resulted in discovery of the Umiat field in 1946 (see Herriott and others, 2018). Linc Energy recently (2013–2014) drilled two additional wells at Umiat. One of these, the Umiat 18 (spudded March 10, 2013) successfully cored through the Nanushuk Formation with 100 percent recovery. The core was saturated with oil, but the well would not flow even after extensive production testing.

The Alaska Division of Geological & Geophysical Surveys (DGGS) and Alaska Division of Oil & Gas (DOG) have studied conventional cores from the four NPRA test wells and the Umiat 18 exploration well. The sedimentology of the cores is documented by LePain (2021 [this volume]). As a parallel study, this report documents the sedimentary petrology and reservoir quality of the Nanushuk siltstone and sandstone encountered in the wells. To augment the subsurface data, petrographic analyses of Nanushuk sandstone collected over several years from measured outcrop sections on the central North

[1]Alaska Division of Oil & Gas, 550 W. 7th Ave., Suite 800, Anchorage, AK 99501-3560; helmold@alaskan.com
[2]Alaska Division of Geological & Geophysical Surveys, 3354 College Rd., Fairbanks, Alaska 99709-3707.
david.lepain@alaska.gov

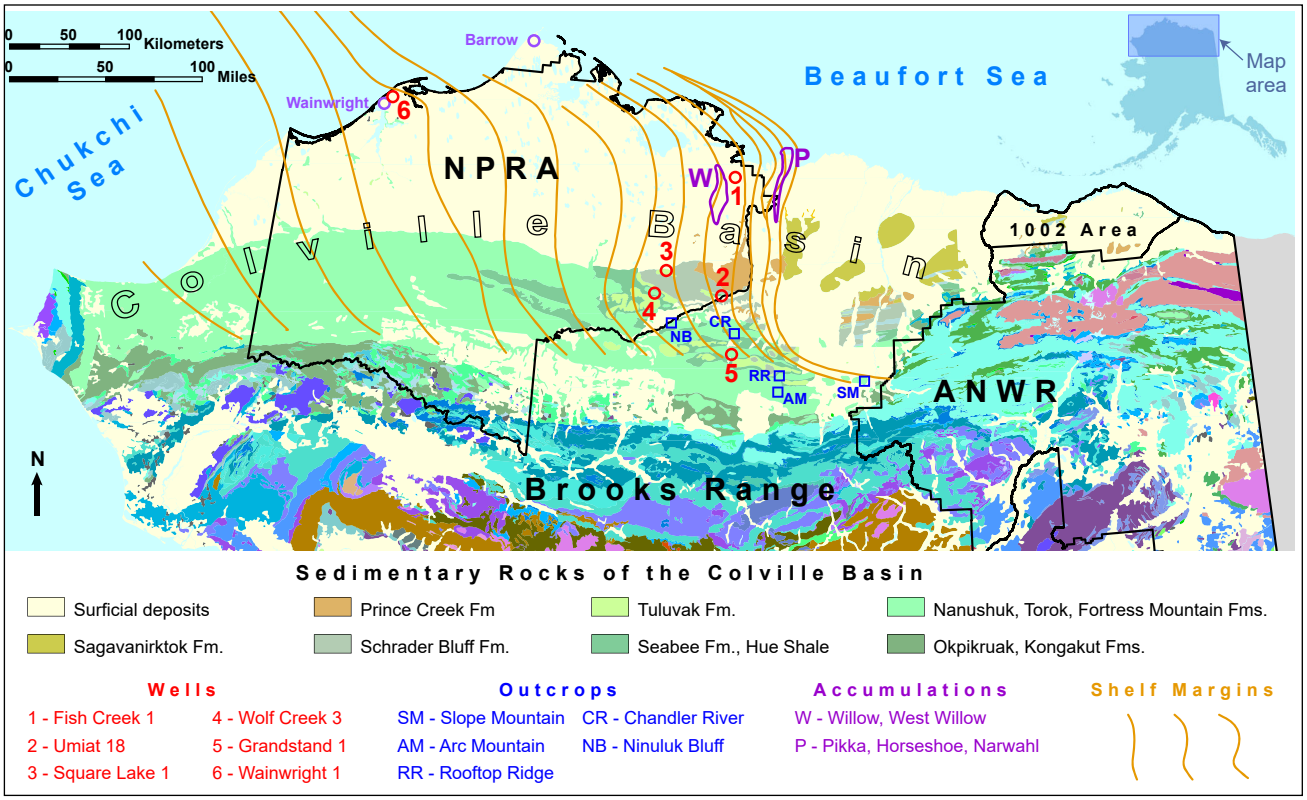

Figure 1. Geologic map of northern Alaska (from Wilson and others, 2015) showing the location of cored wells and measured outcrop sections addressed in this report. Red circles correspond to wells: 1–Fish Creek 1, 2–Umiat 18, 3–Square Lake 1, 4–Wolf Creek 3, 5–Grandstand 1, 6–Wainwright 1; blue squares indicate outcrop sections: SM–Slope Mountain, AM–Arc Mountain, RR–Rooftop Ridge, CR–Chandler River, NB–Ninuluk Bluff. Purple ovals show the locations of the Willow and West Willow (W) and Pikka, Horseshoe, and Narwahl (P) accumulations. Orange lines delineate the approximate locations of Nanushuk lowstand shelf margins (from Houseknecht, 2019).

Slope were incorporated in this study. They proved useful in deciphering the provenance of Nanushuk sandstone. These sedimentologic and petrographic data will advance the understanding of factors that influence hydrocarbon exploration for undiscovered Nanushuk resources.

REGIONAL FRAMEWORK

The Nanushuk Formation outcrops in a belt 30–50 km wide and roughly 650 km long in the northern foothills of the Brooks Range (fig. 1). It consists of a thick succession of marine, transitional, and nonmarine strata of Albian to Cenomanian age (fig. 2) deposited in the asymmetrical Colville foreland basin. The Nanushuk includes a lower, dominantly marine succession of shale, siltstone, and sandstone deposited in shelf, deltaic, and shoreface settings. The lower unit is gradationally overlain by a dominantly nonmarine succession of mudstone, coal, sandstone, and conglomerate deposited in lower delta plain and alluvial settings (Huffman and others, 1985; Mull and others, 2003; LePain and others, 2009). Together these units form a thick regressive package punctuated by higher-frequency marine transgressions resulting from channel avulsion and subsidence of the abandoned delta lobes (LePain and others, 2009) and episodic pulses of basin subsidence (Molenaar, 1985). The uppermost beds of the Nanushuk in the northern part of the outcrop belt and in some wells (Square Lake 1) consist of a Cenomanian mixed marine, marginal-marine, and nonmarine succession deposited during a regional transgressive episode. The transgression culminated in termination of fluvial and deltaic deposition and the re-establishment of widespread marine shelf conditions

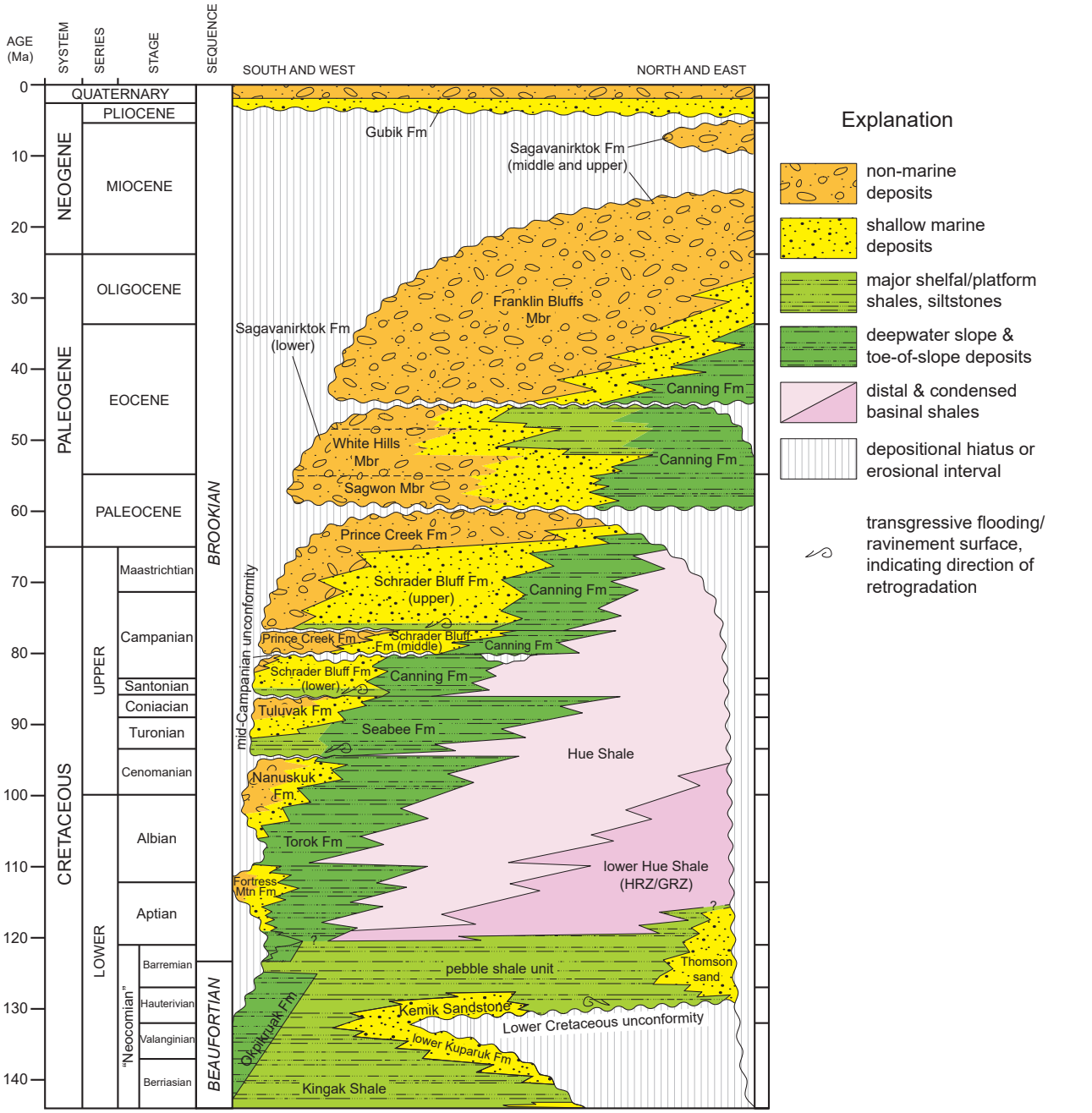

Figure 2. Chronostratigraphic column for the Colville basin, Alaska, showing the stratigraphic position of the Nanushuk Formation; revised from Mull and others (2003), Garrity and others (2005), Decker (2010), and Gillis and others (2014). Abbreviations as follows: Fm = Formation; Mbr = Member; Mtn = Mountain; HRZ = Highly radioactive zone; GRZ = Gamma-ray zone.

throughout the central and western North Slope, and deposition of the Turonian Seabee Formation (Molenaar, 1985; LePain and others, 2009).

Regional studies suggest Nanushuk deposition occurred in two large deltaic complexes separated by the north–south-trending Meade arch (Ahlbrandt and others, 1979; Huffman and others, 1985). The Corwin delta complex (fig. 3) is west of the arch and was interpreted to be the product of a river-dominated system (Ahlbrandt and others, 1979; Huffman and others, 1985). It was sourced from a large drainage basin that extended west of

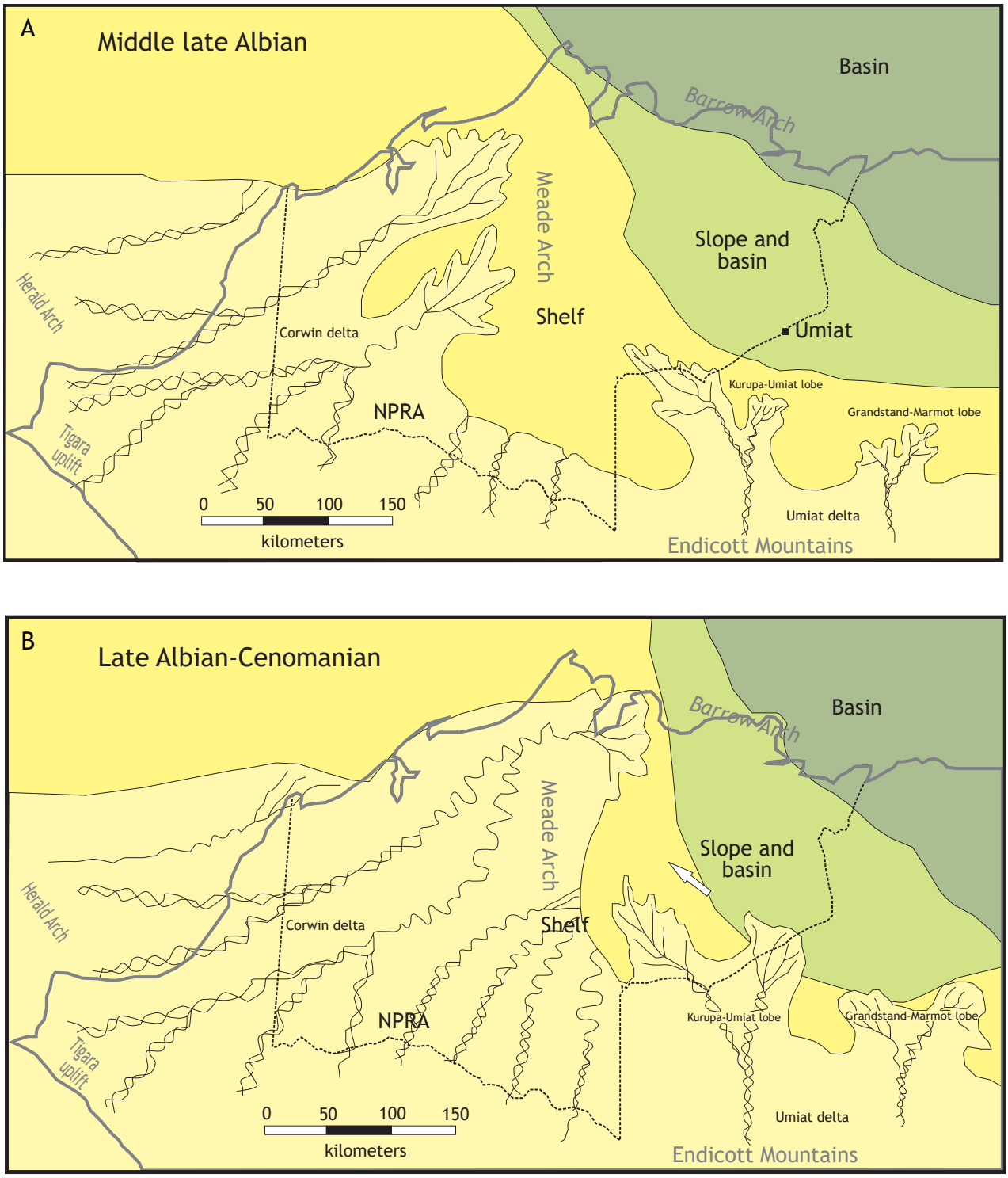

Figure 3. Paleogeographic reconstruction of the central and western Colville basin during (**A**) middle to late Albian time and (**B**) late Albian to Cenomanian time. Diagrams show schematic representation of the Corwin delta west of the Meade Arch and the Umiat delta, including the Kurupa–Umiat and Grandstand–Marmot lobes, east of the arch. Modified from LePain and others (2009) and Huffman and others (1985).

present-day Arctic Alaska (Molenaar, 1985). East of the arch, the Umiat delta complex is comprised of a western Kurupa–Umiat lobe and an eastern Grandstand–Marmot lobe (fig 3). These lobes were recognized as river-dominated systems with a greater degree of wave influence (Ahlbrandt and others, 1979; Huffman and others, 1985) and have been reinterpreted as wave-modified to wave-dominated deltas (LePain and Kirkham, 2001; LePain and others, 2009). They were fed by north-flowing rivers draining smaller catchment areas in the ancestral Brooks Range to the south and southwest (Huffman and others, 1985; LePain and others, 2009). Early Cretaceous uplift of the Brooks Range resulted in clastic detritus shed into the foreland basin from southern sources. The resulting deposits include the deepwater to nonmarine Fortress Mountain Formation, deepwater turbidites of the Torok Formation, and coeval shallow marine to nonmarine strata of the Nanushuk Formation. Some Nanushuk detritus was also probably recycled from the slightly older Fortress Mountain Formation, which was likely sourced exclusively in the ancestral Brook Range to the south (Molenaar and others, 1988; Crowder, 1989; Wartes, 2008). The Torok and Nanushuk Formations collectively represent the transition from an underfilled to an overfilled basin (LePain and others, 2009), with Nanushuk strata eventually over-topping the rift shoulder (Barrow arch) in the late Albian (Molenaar, 1985). The collective Nanushuk deltaic deposits, along with coeval slope and basinal deposits of the Torok Formation, fill the western portion of the Colville basin (Houseknecht and Schenk, 2001; Houseknecht and others, 2008).

Initial work on the petrology of these deltaic systems by Bartsch-Winkler (1979, 1985), Bartsch-Winkler and Huffman (1988), and Johnsson and Sokol (2000) emphasized mineralogy, reservoir quality, provenance, and petroleum potential. Reservoir quality of the Nanushuk sandstone was previously investigated by Fox (1979), Fox and others (1979), Reifenstuhl and Loveland (2004), and Shimer and others (2014).

DATASETS AND METHODS

Two datasets were utilized for this report: modal data and routine core analyses (RCA). The modal data were obtained by point counting existing thin sections from the four 1950's-vintage U.S. Navy test wells that are archived at the Alaska Geological Materials Center (GMC) in Anchorage and more recent vintage (2013) thin sections from the Umiat 18 conventional cores. To aid the assessment of provenance, modal data were also obtained from thin sections collected from five outcrop sections in the central North Slope. The routine core analyses consist largely of legacy data for conventional cores from the four U.S. Navy test wells (Robinson, 1958; Collins, 1959; Robinson and Collins, 1959), a small secondary dataset from Grandstand 1, and more recent (2013) analyses of Umiat 18 conventional cores that were commissioned by Linc Energy. The routine core analyses for Umiat 18 were performed by Weatherford Laboratories and obtained from the Linc Energy data archivist. Recent analyses of petrophysical properties (porosity, permeability, grain density) are available for many of the outcrop samples.

Modal Analyses

GMC's thin-section collection was mined for existing thin sections from the four U.S. Navy test wells that covered the stratigraphic intervals described by LePain (2021 [this volume]). Initial cursory examination of 111 thin sections—21 from Fish Creek 1, 23 from Square Lake 1, 41 from Grandstand 1, and 26 from Wolf Creek 3—revealed they are of widely varying quality and of different vintages. Many of the older thin sections are not impregnated with blue-dyed epoxy, a procedure that is currently accepted as standard protocol to aid in the recognition of porosity. Other thin sections are severely plucked or wedged rendering them unsuitable for further analysis. The extent and quality of staining also are highly variable. Only a few thin sections are stained for K-feldspar and virtually none for carbonate minerals. Sixty-six thin sections that are impregnated with blue-dyed epoxy and which

display minimal plucking or wedging were deemed of acceptable quality for more detailed analysis: 10 from Fish Creek 1, 13 from Square Lake 1, 26 from Grandstand 1, and 17 from Wolf Creek 3. They are listed in appendix A.

Forty-one thin sections from the Umiat 18 conventional cores were obtained from Linc Energy. They are of high quality and are both impregnated with blue-dyed epoxy and stained for carbonates; a small subset is also stained for plagioclase. Thirty-eight of the thin sections were deemed suitable for modal analysis; they are listed in appendix A. The three samples that were not analyzed consist of mudstone and are too fine grained to point count.

Modal analyses of the 104 samples were performed by Michael D. Wilson of Wilson & Associates. He counted a minimum of 300 points using the traditional (non-Gazzi–Dickinson) point-counting method (Ingersoll and others, 1984; Decker and Helmold, 1985) to determine the composition of the framework (detrital grains) and intergranular (matrix, cement, porosity) components. The modal analyses are presented in two formats: (1) raw counts by Wilson (app. B), and (2) standardized hierarchical categories originally devised by Decker (1985) and subsequently modified by the senior author to include additional categories (app. C). All interpreted data, plots, and tables in this report are based on the Decker–Helmold system. Summaries of the modal data, standard petrologic parameters, and ternary ratios are presented in appendix D, and petrographic ratios used to construct ternary diagrams are listed in appendix E.

Wilson conducted a second count of 200 grains (including matrix) for grain size. A complete listing of the grain-size data in both millimeter and ϕ (phi) units is presented in appendix F. The original composition and grain-size files provided by Wilson and a file containing the composition data in Decker–Helmold format are available from the DGGS website (https://doi.org/10.14509/30728).

To facilitate provenance determination, this report also includes existing modal analyses of fifty Nanushuk thin sections from the DGGS/DOG petrographic database. The represented samples had been collected over a period of several years from five measured outcrop sections on the central North Slope: 15 from Slope Mountain, 10 from Arc Mountain, 3 from Rooftop Ridge, 5 from Chandler River, and 17 from Ninuluk Bluff. The thin sections are of high quality and are impregnated with blue-dyed epoxy and stained for carbonates. The modal analyses were performed by Michael D. Wilson shortly after the samples were collected following the procedure outlined above but have not previously been published. The analyses are detailed in appendices A–F.

Routine Core Analyses

Contemporary studies of sandstone reservoir quality routinely utilize thin sections made from trim ends of core plugs destined for routine core analyses. This ensures good correlation between petrologic parameters (detrital grain composition, cement abundance, rock texture) and reservoir rock properties (porosity, permeability, grain density). This study utilizes two disparate sets of routine core analyses: legacy data dating back to 1959 that do not meet the above criteria, and more recent data circa late 1980's and 2013 that do. Available core analyses of the four test wells date back to the original evaluations of the cores by the U.S. Geological Survey (Collins, 1959; Robinson and Collins, 1959), and consist of measurements of permeability to air and porosity under ambient conditions. Very few of the thin sections point counted for this study have corresponding measurements of porosity and permeability in the legacy RCA data. The sampling depths for porosity and permeability are reported to the nearest foot, while the locations of the thin sections are typically recorded to the nearest tenth or hundredth of a foot. As a result, it cannot be ascertained whether RCA data acquired at any given depth are from the same piece of rock used to make the thin sections. Discrepancies of as little as one tenth of a foot are enough to call into question the degree of correlation between the RCA and point-count data. Further, some of the thin sections are

rectangular in shape, suggesting they were not cut from cylindrical RCA plugs that have a round cross section. Appendix G lists a total of 240 analyses have been compiled from Fish Creek 1 (2 analyses), Square Lake 1 (54 analyses), Grandstand 1 (123 analyses), and Wolf Creek 3 (61 analyses).

Routine core analyses from the late 1980's are available for 14 samples from the Grandstand 1 well. These data consist of measurements of permeability to air and porosity under ambient conditions (app. G). The data were obtained from plugs cut from the core stored at the Alaska Geological Materials Center (GMC), which at the time was in Eagle River, AK. Unfortunately, modal analyses of thin section cut from the analyzed plugs are not available for publication.

For the Umiat 18 well, Linc Energy provided routine core analyses of 72 samples that were performed by Weatherford Labs in 2013 (app. G). These measurements include permeability to air and calculated Klinkenberg equivalent values, and porosity measured under a net confining stress of 300 psi and under ambient conditions. Because the Umiat thin sections were cut from the analyzed core plugs there is good correlation between the petrographic and routine core datasets.

Analyses of petrophysical properties (porosity, permeability, grain density) performed by Weatherford Laboratories are available for 38 central North Slope outcrop samples (app. G). These measurements include air permeability, calculated Klinkenberg values, ambient porosity, and porosity under a net confining stress of 400 psi.

To integrate data from both the legacy and recent routine core analyses in scatter plots and discussions, the rudimentary measurements of permeability to air and ambient porosity are utilized throughout this report.

PETROLOGIC FACIES

Grouping samples into petrologic facies (petrofacies) helps summarize data, decipher trends, and describe groups with similar characteristics. Samples from the five NPRA wells were assigned to petrofacies with the aid of DataDesk, a statistical software application produced by Data Description, Inc. (Velleman, 1998). Due to the lack of correlation between the modal and routine core data (see above), these two datasets were analyzed independently. Variables describing texture (e.g., grain size, sorting) and composition (e.g., grain types, matrix, cement) were amassed into one database; while variables describing reservoir quality (e.g., porosity, permeability, burial depth) were compiled into a second database.

Evaluation of rock texture and composition ascertained from detrital modes reveals natural grouping of the data based on grain size. Similar trends in mineralogy versus grain size (e.g., chert vs grain size) were observed for all five NPRA wells. As a result, the modal data were grouped into three petrofacies based on grain size: siltstone petrofacies (21 samples), very-fine-grained sandstone petrofacies (36 samples), and fine-grained sandstone petrofacies (47 samples). Two medium-grained sandstones (Umiat 18, 769 ft measured depth and Grandstand 1, 902 ft measured depth) were included in the fine-grained sandstone petrofacies to avoid having a group based only on two samples. Their average grain sizes—1.93 phi (0.26 mm) for Umiat 18 and 1.90 phi (0.27 mm) for Grandstand 1—are close to the 2.0 phi (0.25 mm) lower boundary of medium-grained sand, so their inclusion in the fine-grained sandstone petrofacies is easily justified. To assess how the composition of these petrofacies compare to Nanushuk sandstone across the North Slope, data from 30 exploration and test wells (table 1) are included in the ternary plots for comparison (fig. 4) and are hereafter referred to as regional Nanushuk data. The petrology and reservoir quality of Nanushuk sandstone in one of these wells, the USGS Wainwright test well 1 (Wainwright 1 in table 1), is documented in Helmold (2016) and is highlighted throughout the text and figures of this report were relevant.

Evaluation of reservoir quality (porosity, permeability, burial depth) reveals natural grouping

Table 1. Exploration and test wells for which point-count data are available for Nanushuk sandstone. These 30 wells comprise the regional Nanushuk data addressed in this report.

Ord	Operator	Well	API	Top Zone (feet)	Base Zone (feet)	N	Erosion (feet)
1	Arco	Alpine 1	50103202110000	4046.00	4535.00	4	1176
2	US Navy	Barrow Core Test 1	50023100050000	169.00	194.00	6	2725
3	Arco	Big Bend 1	50287200110000	1100.00	2840.00	9	8002
4	Husky	E Simpson 2	50279200070000	2387.00	2398.00	9	1785
5	Arco	Fiord 2	50103202010000	4828.00	4828.00	1	844
6	Arco	Hunter A	50103204050000	3625.00	3652.00	7	2068
7	Husky	Inigok 1	50279200030000	2632.00	3081.90	7	3223
8	US Navy	Knifeblade 1	50119100120000	312.00	1490.00	6	6777
9	BP	Kuparuk Unit 1	50287100180000	5529.00	5930.00	9	7090
10	Sinclair	Little Twist Unit 1	50287100220000	942.00	3611.00	4	8895
11	US Navy	Meade 1	50163100020000	1795.00	2950.00	2	4560
12	Arco	Nanuk 2	50103203320000	4796.00	4828.00	3	1381
13	US Navy	Oumalik Test 1	50119100050000	916.00	2758.30	17	4711
14	ConocoPhillips	Putu 2A	50103207630100	4293.40	4361.25	10	1531
15	Husky	Seabee 1	50287200070000	270.00	2120.00	7	6564
16	ConocoPhillips	Tinmiaq 2	50103207300000	3311.00	3766.50	45	1650
17	ConocoPhillips	Tinmiaq 6	50103207310000	2450.00	3824.00	56	1418
18	US Navy	Topagoruk 1	50279100330000	302.00	2097.00	10	2748
19	BP	Trailblazer A1	50103203640000	2972.00	3454.00	4	1402
20	BP	Trailblazer H1	50103203690000	2760.00	3090.00	3	1525
21	Texaco	Tulugak 1	50057200010000	1460.00	2540.00	4	8030
22	Husky	Tunalik 1	50301200010000	3288.00	5560.60	3	3036
23	Union	Tungak Ck 1	50207200020000	3067.00	4661.00	10	4979
24	US Navy	Umiat Test 1	50287100010000	1335.00	2996.00	6	6614
25	US Navy	Umiat Test 2	50287100020000	413.00	969.00	4	6469
26	US Navy	Umiat Test 7	50287100070000	834.00	1370.00	5	6543
27	US Navy	Umiat Test 8	50287100080000	507.00	711.00	2	6374
28	US Navy	Umiat Test 11	50287100110000	2048.00	3004.00	37	6301
29	USGS	Wainwright 1	50301200030000	181.15	1501.45	48	2762
30	US Navy	Wolf Ck 2	50119100090000	2511.00	3520.00	20	7071

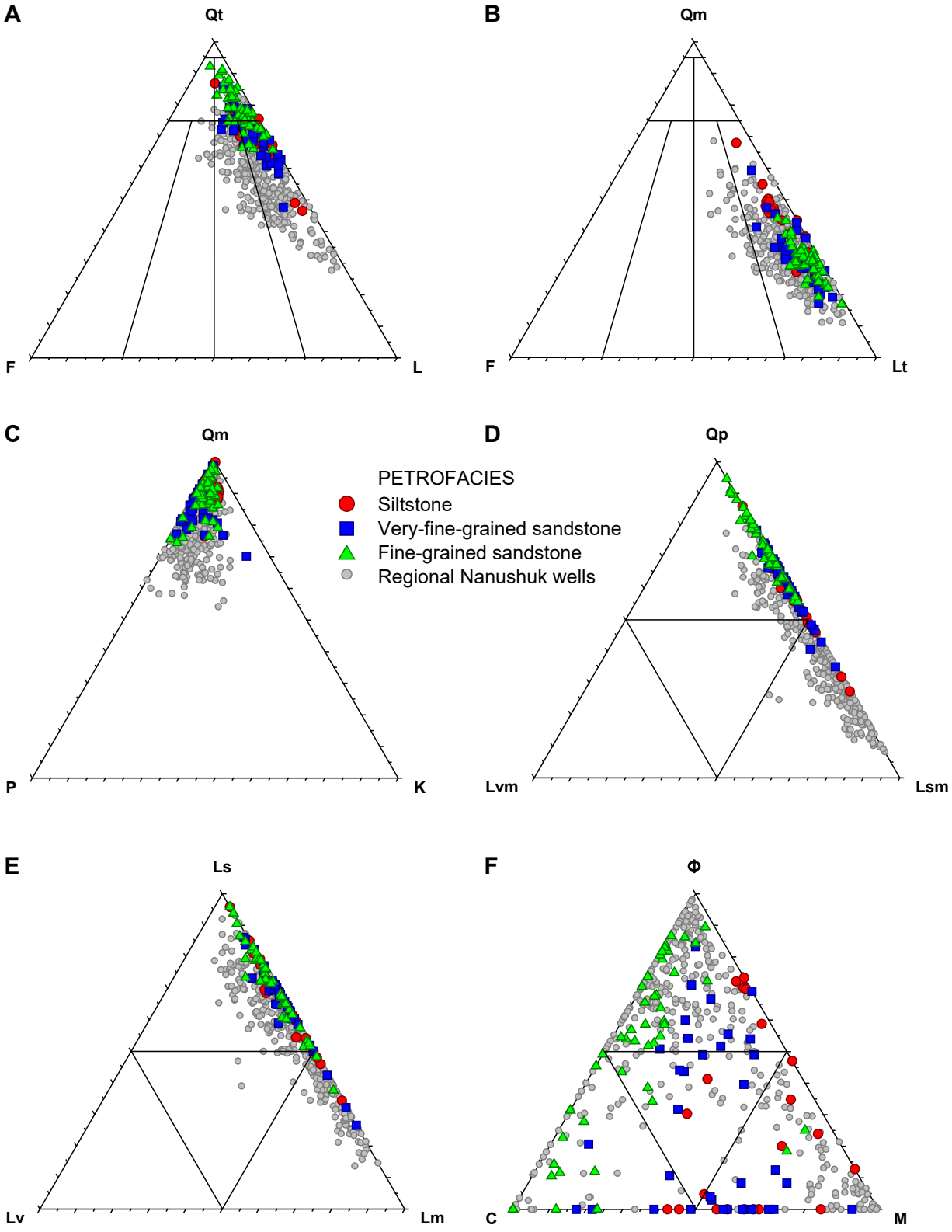

Figure 4. Ternary diagrams showing composition of Nanushuk sandstone. The data were obtained via the traditional point-counting method in which phaneritic rock fragments are classified by their lithology (for example, granite, diorite, gabbro, gneiss). Colored symbols represent petrofacies from the five NPRA wells in this study; gray circles represent regional Nanushuk wells (table 1). See table 2 for explanation of grain and intergranular parameters used in the diagrams. (**A**) QtFL diagram; (**B**) QmFLt diagram; (**C**) QmPK diagram; (**D**) QpLvmLsm diagram; (**E**) LsLvLm diagram; (**F**) ΦCM diagram.

of the data by well. Sandstone in wells that have undergone deeper burial tend to have lower porosity and permeability. As a result, data in plots illustrating trends in reservoir quality are coded by well.

To summarize, this report groups samples differently depending on the type of data under discussion: diagrams dealing with mineral composition (e.g., ternary plots) are coded by grain size, those dealing with reservoir quality are coded by well.

Siltstone Petrofacies

The siltstone petrofacies is represented by 21 samples typically consisting of laminated siltstone with a variable matrix content. The samples have an average modal composition of $Qt_{71}F_4L_{25}$, $Qm_{41}F_4Lt_{55}$, $Qm_{91}P_6K_3$, $Qp_{57}Lvm_0Lsm_{43}$ (fig. 4, app. E, table 2), and a plagioclase/total feldspar (P/F) ratio of 0.71. The average grain size (fig. 5, app. F) of the siltstone is 0.047 mm (coarse silt), with an average Folk sorting (Folk, 1974) of 1.78 (poor). The siltstone framework composition is somewhat different from the sandstone largely due to the difference in grain size (see section on petrologic trends). Monocrystalline quartz (Qm) and polycrystalline quartz (Qp) are the two most abundant detrital grains, averaging 37 percent and 15 percent of the framework fraction, respectively (fig. 6). Feldspar is a minor framework component (average 4 percent), consisting of roughly equal proportions of plagioclase and K-feldspar. The lithic fraction consists largely of chert (average 13 percent), phyllite/schist (average 11 percent), detrital carbonate (average 6 percent), and shale/mudstone (average 4 percent). Volcanic rock fragments (VRFs) and quartzite are minor lithic components. Micas (average 3 percent) and organic material (average 3 percent) are more abundant

Table 2. Classification of grain and intergranular parameters used in ternary diagrams (fig. 4).

A. Quartzose grains

Qm = Monocrystalline quartz

Qp = Polycrystalline quartz (including chert)

Qt = Total quartzose grains (Qm + Qp)

B. Feldspar grains

P = Plagioclase

K = Potassium feldspar

F = Total feldspar grains (P + K)

C. Lithic grains

Ls = Sedimentary rock fragments (including chert)

Lv = Volcanic rock fragments

Lm = Metamorphic rock fragments

Lp = Plutonic rock fragments

Lsm = Sedimentary and metasedimentary rock fragments

Lvm = Volcanic and metavolcanic rock fragments

L = Lithic grains (Ls + Lv + Lm + Lp)

Lt = Total lithic grains (L + Qp)

D. Intergranular components

Φ = Total porosity

C = Total cement

M = Matrix + clay laminae/burrows

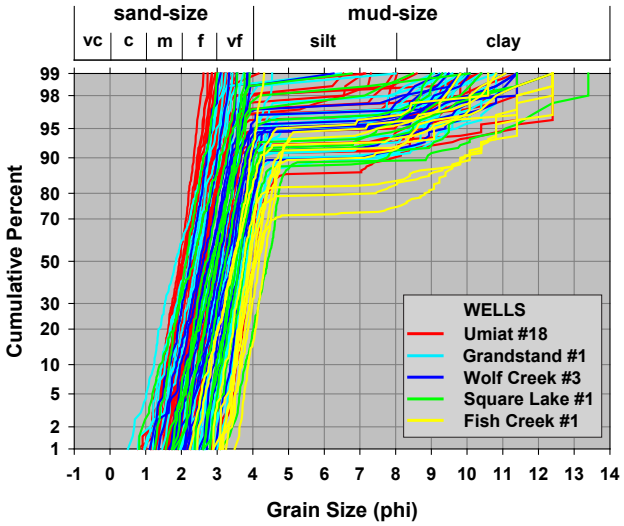

Figure 5. Cumulative probability plots of grain size by well; each line represents an individual sample. Sediment with a normal (Gaussian) distribution plot as a straight line; tails to the right indicate a significant mud (silt and clay) fraction. The value of the 50th percentile indicates the median grain size, while sorting is denoted by the slope of the line.

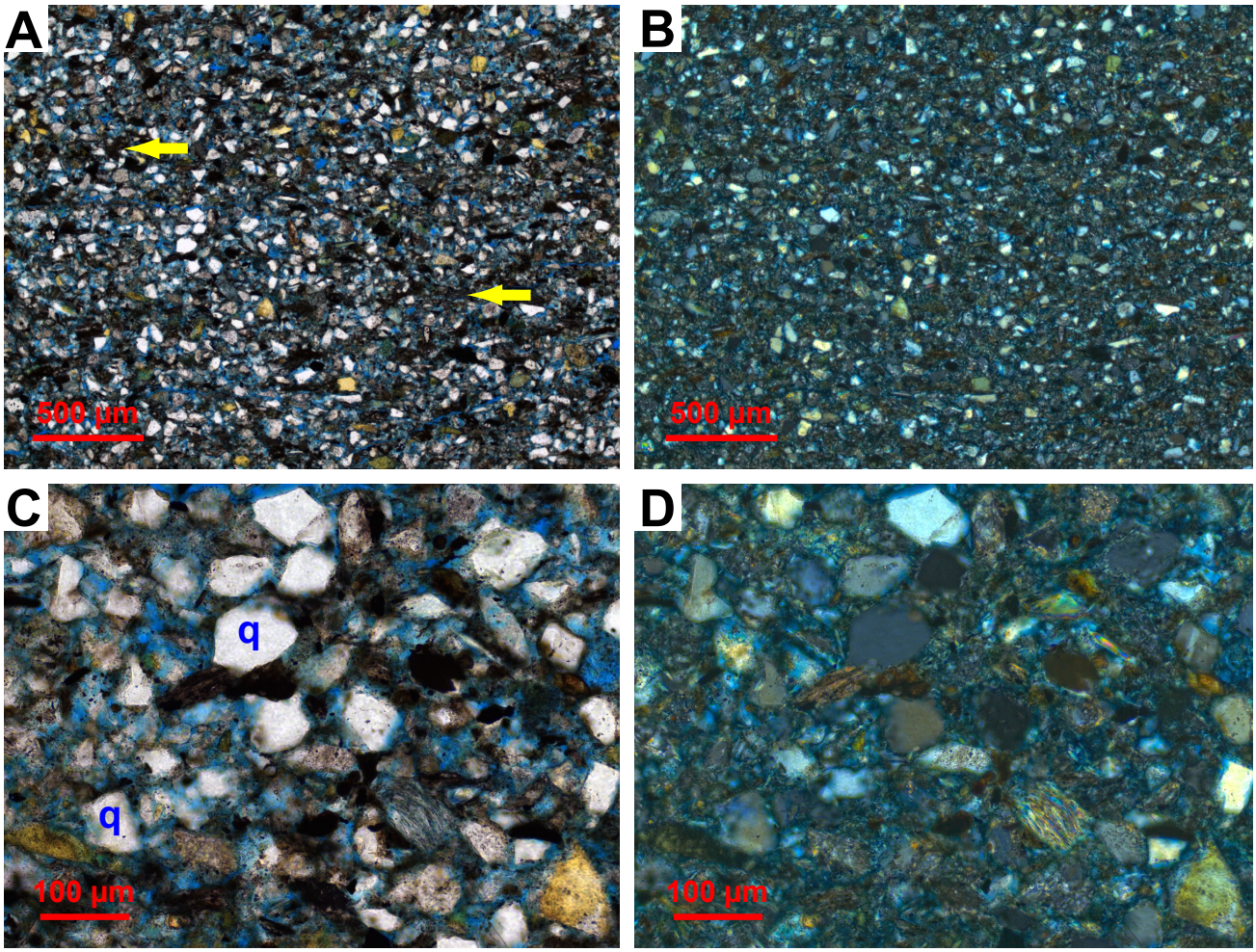

Figure 6. Photomicrographs of siltstone petrofacies. (**A**) General view of siltstone showing an abundance of detrital clay (arrows). Plane-polarized light; Fish Creek 1, 3,025.9 ft. (**B**) Same view as A. Crossed polars; Fish Creek 1, 3,025.9 ft. (**C**) Detailed view of siltstone in which the framework fraction consists largely of monocrystalline quartz (q). Plane-polarized light; Fish Creek 1, 3,025.9 ft. (**D**) Same view as C. Crossed polars; Fish Creek 1, 3,025.9 ft.

than in the sandstones, due to their hydrodynamic equivalence with the finer detritus.

Thin-section porosity averages 6.3 percent but varies widely between samples (0–19 percent). Detrital clay matrix is a prominent intergranular component (average 11 percent) that negatively impacts reservoir quality, particularly permeability. Quartz cement is negligible in all samples, but carbonate cement is present in a few samples (0–14 percent of bulk rock, average 3 percent). Intergranular volume (IGV), which is defined as the sum of intergranular porosity, intergranular cement, and depositional matrix (Szabo and Paxton, 1991; Paxton and others, 2002) and is an indicator of degree of compaction, ranges from 13 to 33 percent suggesting a wide range in compaction resulting from large differences in maximum burial depths (see discussion of reservoir quality).

Very-Fine-Grained Sandstone Petrofacies

The very-fine-grained sandstone petrofacies is represented by 36 litharenites with an average modal composition of $Qt_{70}F_5L_{25}$, $Qm_{31}F_5Lt_{64}$, $Qm_{86}P_{11}K_3$, $Qp_{62}Lvm_0Lsm_{38}$ (fig. 4, app. E, table 2), and plagioclase/total feldspar (P/F) ratio of 0.86. Their average grain size (fig. 5, app. F) is 0.088 mm (upper very fine), with an average Folk sorting (Folk, 1974) of 1.33 (poor). Monocrystalline and polycrystalline

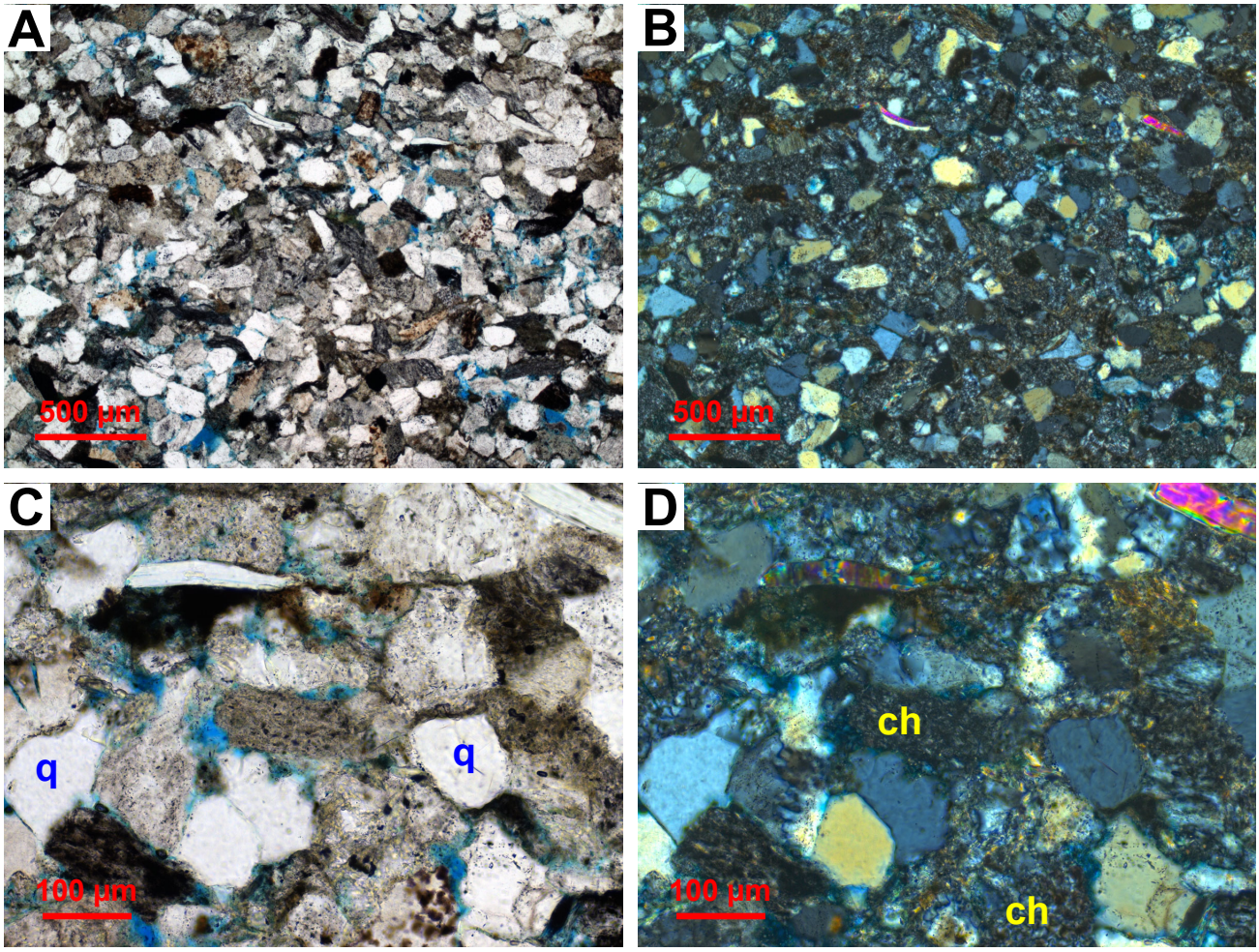

Figure 7. Photomicrographs of very fine-grained sandstone petrofacies. (**A**) General view showing a moderately compacted framework lacking significant cement. Plane-polarized light; Square Lake 1, 3,058 ft. (**B**) Same view as A. Crossed polars; Square Lake 1, 3,058 ft. (**C**) Detailed view of sandstone showing abundance of monocrystalline quartz (q). Plane-polarized light; Square Lake 1, 3,058 ft. (**D**) Same view as C. Note chert grains (ch). Crossed polars; Square Lake 1, 3,058 ft.

quartz are the two dominant framework components, averaging 29 percent and 17 percent of the framework fraction, respectively (fig. 7). Feldspar is a minor framework component, averaging 4 percent plagioclase and 1 percent K-feldspar. Lithic detritus consists largely of chert (20 percent), phyllite/schist (13 percent), detrital carbonate (4 percent), shale/mudstone (4 percent), and quartzite (2 percent). Organic matter (3 percent) and micas (2 percent) are accessory detrital components.

Thin-section porosity averages 4 percent and like the siltstone petrofacies exhibits substantial inter-sample variability (0–19 percent). Quartz (average 1 percent) and carbonate (average 3 percent) are minor cements in most samples, but carbonate cement ranges up to 10 percent in a few samples. Kaolinite occurs in trace quantities as a patchy, pore-filling cement. Detrital matrix ranges from 1 to 11 bulk percent (average 5 percent) and is locally concentrated along diffuse laminae. Intergranular volume (IGV) ranges from 8 to 26 percent (average 13 percent) suggesting the samples have undergone a range of compaction from moderate to significant.

Fine-Grained Sandstone Petrofacies

The fine-grained sandstone petrofacies is represented by 47 chert-rich litharenites with an average modal composition of $Qt_{79}F_4L_{17}$, $Qm_{30}F_4Lt_{66}$,

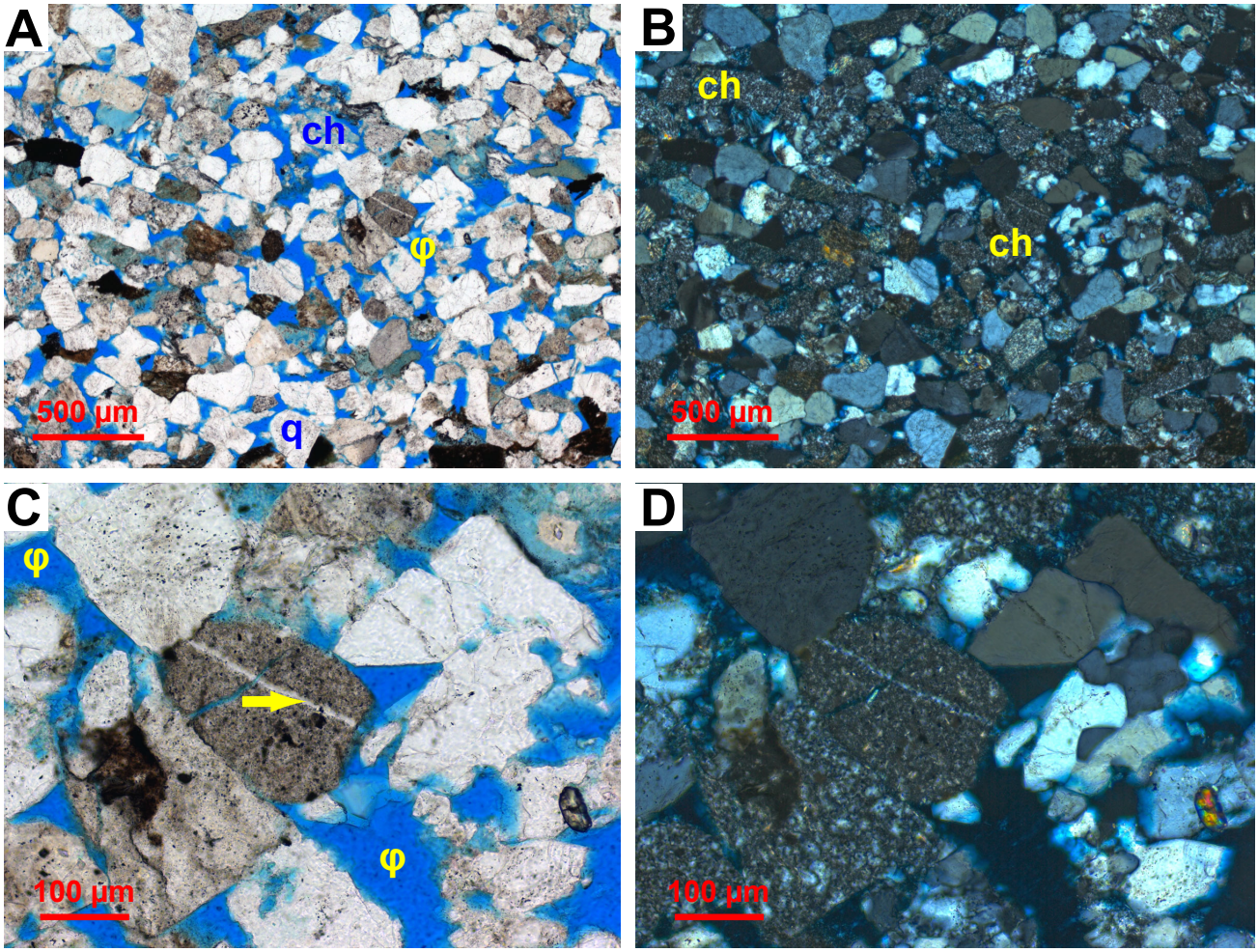

Figure 8. Photomicrographs of fine-grained sandstone petrofacies. (**A**) General view showing abundance of quartz (q) and chert (ch) which is best seen under crossed polars. Note abundant intergranular pores (ϕ). Plane-polarized light; Umiat 18, 803.05 ft. (**B**) Same view as A showing abundant chert grains (ch). Crossed polars; Umiat 18, 803.05 ft. (**C**) Detailed view showing common intergranular pores (ϕ). Note fractured chert grain with quartz veinlet (arrow). Plane-polarized light; Umiat 18, 803.05 ft. (**D**) Same view as C. Crossed polars; Umiat 18, 803.05 ft.

$Qm_{89}P_9K_1$, $Qp_{74}Lvm_0Lsm_{26}$ (fig. 4, app. E, table 2), and plagioclase/total feldspar (P/F) ratio of 0.77. The average grain size (fig. 5, app. F) is 0.186 mm (upper fine), with an average Folk sorting (Folk, 1974) of 0.67 (moderate). Chert and monocrystalline quartz (Qm) with dominantly straight to slightly undulose extinction are the two dominant framework components, each averaging 29 percent of the framework fraction (fig. 8). Chert is largely of the common microcrystalline variety, although micaceous-argillaceous and micro-porous chert also occur. Polycrystalline quartz (Qp) averages 17 percent of the detrital framework and consists of grains with 2–5 crystals (plutonic and high-rank metamorphic provenance) and grains with more than 5 crystals (low-rank metamorphic provenance; Basu and others, 1975; Blatt and others, 1980; Blatt, 1982; Boggs, 2009). Feldspar comprises roughly 4 percent of the framework with plagioclase—some of which exhibit minor to moderate dissolution—more abundant than K-feldspar. Lithic fragments (excluding chert) comprise approximately 17 percent of the rock framework, consisting of phyllite/schist, quartzite, and detrital carbonate. Micas, heavy minerals, and dispersed organic grains occur in trace amounts.

Thin-section porosity averages 9.2 percent, and like the other petrofacies, exhibits substantial

inter-sample variability (0–20 percent). Quartz (average 3 percent) and carbonate (average 3 percent) are minor cements in most samples, but carbonate cement ranges up to 35 percent in a few samples. Kaolinite is a patchy, pore-filling cement that occurs in trace quantities. The samples exhibit a wide range of IGV (1–39 percent, average 17 percent) suggesting the five wells experienced substantial differences in compaction.

GRAIN-SIZE TRENDS

The Nanushuk siltstone and sandstone in the five NPRA wells exhibit a positive correlation between chert content and grain size (correlation coefficient of -0.76), with the fine-grained sandstone averaging 24 percent (whole rock) chert while the siltstone averages over 10 percent (fig. 9A). It should be noted that because grain size is given in phi (ϕ) which is defined as $-\log_2(\text{grain size}_{mm})$, a positive correlation between variables (e.g., chert content increases with increasing grain size) is reported as a negative value of the Pearson product-moment correlation coefficient (r). To best display the relationship between chert content and grain size, the ordinate (chert content) on the cross-plot (fig. 9A) is displayed using a logarithmic scale with a corresponding increase of r to -0.80. A similar trend was noted in Nanushuk siltstone and sandstone in the Wainwright 1 test well (Helmold, 2016). The regional, subsurface Nanushuk sandstone samples (gray dots in fig. 9A, table 1) display a similar, although weaker, correlation suggesting the grain size versus chert relationship may be characteristic of Nanushuk sandstone. A possible explanation may lie in the source of the chert grains (Helmold, 2016). One of the more likely chert sources is the Mississippian-Pennsylvanian Lisburne Group carbonates that are widespread in the allochthons of the Brooks Range. These carbonates contain ubiquitous, large (cobble- to boulder-sized), bed-parallel, diagenetic chert nodules. As these nodules weather and erode from the Lisburne, they are concentrated in the coarsest detritus. Abundant silt to very-fine sand-sized chert grains should ultimately be produced with continued transport and abrasion if its solubility is comparable to that of quartz. The higher solubility of chert relative to monocrystalline quartz, combined with the greater surface area of microcrystalline chert, may result in its selective dissolution thereby increasing the relative abundance of quartz in the finer fractions (Helmold, 2016). A similar relationship between chert content and grain size is also seen in Ivishak sandstones from the North Slope of Alaska where the chert content is thought to be related to distance of transport (Atkinson and others, 1990). The coarsest detritus, having undergone little transport, contains a significant volume of chert. In the finer detritus that was transported greater distance, chert was selectively removed through abrasion relative to the more resistant monocrystalline quartz. The correlations of grain size with Qm (+ r value) and VRFs (- r value) observed in Nanushuk siltstone and sandstone from the Wainwright 1 test well (Helmold, 2016) were not evident in the current study.

A relationship between grain size and reservoir quality (porosity, permeability) is illustrated by Umiat 18 where thin sections were cut from the routine core plugs. Twenty-three (23) of the point-counted samples have corresponding porosity and permeability measurements, while one additional sample has only a porosity measurement. Two fine-grained sandstones were considered outliers and excluded from analysis; one (942.0 ft measured depth) was excluded due to excessive carbonate cement (12 percent), the other (811.6 ft measured depth) was excluded due excess detrital matrix (9 percent). There is a well-defined positive correlation between grain size and porosity for the Umiat 18 samples, with a Pearson product–moment correlation coefficient (r) of -0.85 (fig. 9B). The fine- and very-fine-grained sandstone have average porosities of 15 and 11 percent, respectively, while siltstone porosity averages 8 percent. It is difficult to quantify a similar relationship for Fish Creek 1, Square Lake 1, Grandstand 1, and Wolf Creek 3 because few samples from these wells have both grain size and

porosity data due to the lack of correlation between the petrographic and routine core analysis datasets (see above). Sparse data for Grandstand 1 and Wolf Creek 3 appear to approximate a linear relationship (fig. 9B). The entire dataset, including the regional Nanushuk data, clusters into two distinct groups. The first group displays similar ranges in porosity (less than 20 percent) and grain size as the Umiat 18 samples and has Dmax values generally greater than 7,000 ft (red dashed oval in fig. 9B). Samples from Grandstand 1 and Wolf Creek 3 are included in this group. The second group has greater porosities than the Umiat 18 samples for a given grain size, with Dmax values generally less than 7,000

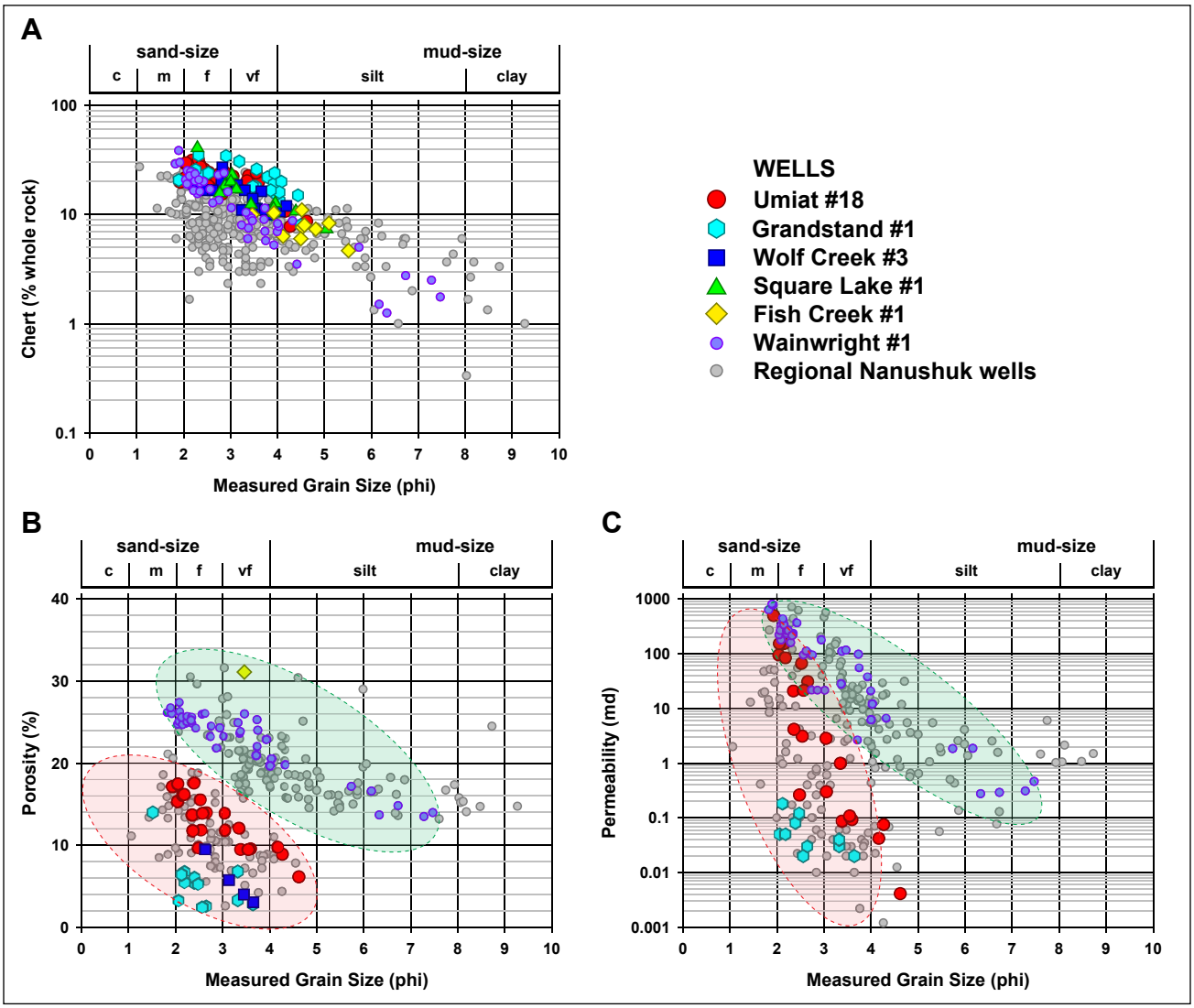

Figure 9. Cross plots of grain size, in phi units (ϕ), versus compositional and petrophysical parameters. Because grain size is given in phi (ϕ) [defined as -log2(grain size mm)], a positive correlation between variables (i.e., permeability increases with increasing grain size) is reported as a negative value of the Pearson product-moment correlation coefficient (r). To best display a linear relationship between variables, the ordinate (y-axis) representing chert is displayed with a logarithmic scale. **A**. Chert – grain size plot showing good correlation for six NPRA wells and regional samples. Chert preferentially resides in the coarser fraction of the detritus. **B**. Porosity – grain size plot showing two linear trends; one for rocks with better reservoir quality (green dashed oval) subjected to shallow to moderate burial, and the other for rocks with poorer reservoir quality (red dashed oval) subjected to moderate to deep burial. **C**. Permeability – grain size plot showing trends similar to the porosity – grain size plot. Rocks with better reservoir quality (green dashed oval) merge with rocks with poorer reservoir quality (red dashed oval) in the coarser detrital faction.

ft (green dashed oval in fig. 9B). Samples from the Wainwright 1 test well and a single sample from Fish Creek 1 are included in the latter group (fig. 9B). These two parallel trends are interpreted to result from differences in burial histories—specifically differences in Dmax, as discussed below.

Umiat 18 samples also display a pronounced positive correlation between grain size and permeability (r = -0.91), with an average permeability of 94 md in the fine-grained sandstone, 0.7 md in the very-fine-grained sandstone, and 0.04 md in the siltstone (fig. 9C). The regional Nanushuk data also cluster into two groups: one typified by the Umiat 18 and Grandstand 1 samples (Dmax > 7,000 ft), the other by the Wainwright 1 samples (Dmax < 7,000 ft). The two groups merge at higher permeability values. The existence of the two groups in the regional data is also interpreted to reflect differences in burial.

PROVENANCE SIGNALS

As detailed above, the detrital framework of Nanushuk sandstone consists largely of monocrystalline and polycrystalline quartz, chert, phyllite/schist, shale/mudstone, and detrital carbonate grains, with lesser quantities of feldspar, volcanic rock fragments, mica, and heavy minerals. Among this detritus, chert and detrital carbonate probably have the most potential to decipher the provenance of specific samples; phyllite/schist detritus could potentially be a useful indicator of provenance if combined with other techniques such as thermochronology of detrital micas, although that is beyond the scope of this report. Nanushuk sandstone in the subsurface of the eastern NPRA was derived from uplifts in the ancestral western Brooks Range, Lisburne Hills/Herald arch, and eastern Siberia (Molenaar, 1985; Houseknecht and others, 2008). The Brooks Range orogen consists of a stack of allochthons that include thick successions of carbonate, bedded chert, and silicified mudstone—many of which extend across the east-west length of the mountain belt and were likely exposed and shedding detritus during Nanushuk deposition. Allochthons that potentially supplied chert and silicified mudstone include the western parts of the Endicott Mountains (Lisburne Group, Kuna Formation, Otuk Formation), Picnic Creek (Lisburne Group-Akmalik Chert, Imnaitchiak Chert), Kelly River (Lisburne Group-Tupik Formation), Ipnavik River (Lisburne and Etivluk Groups), and Nuka Ridge (Etivluk Group; see fig. 21 in Moore and others, 1994).

The lack of carbonate staining of thin sections from the four legacy NPRA test wells hampers definitive identification of carbonate fragments. However, analyses of the state's regional collection of Nanushuk thin sections (which have been stained for carbonate) and Umiat 18 samples suggest that most carbonate fragments are dolomite, with only a small proportion consisting of calcite. Detrital carbonate occurs in variable amounts (0–35 percent of the framework, 0–28 percent of the bulk rock) in the five wells examined in this study, with variability observed both within and between wells (figs. 10A, 11A). Samples from Grandstand 1 and Umiat 18 contain the least detrital carbonate, most having little to none. Those from Square Lake 1, Wolf Creek 3, and Fish Creek 1 contain a much wider range of detrital carbonate (fig. 11A), which is a principal lithic variant in many samples. Previous work demonstrated that Nanushuk sandstone from the Wainwright 1 well also contains significant detrital carbonate (fig 11A; Helmold, 2016). This study appears to show a pattern in aerial distribution of detrital carbonate in the Nanushuk sandstone, although the number of wells was limited. Sandstone to the southeast (Grandstand 1 and Umiat 18) contains relatively little detrital carbonate, while sandstone to the northwest (Wolf Creek 3, Square Lake 1, Fish Creek 1, and Wainwright 1) contains significantly more (figs. 1, 11A). To test the validity of this observation, the abundance of detrital carbonate in Nanushuk sandstone from five measured stratigraphic sections in the central North Slope was compared. Nanushuk sandstone from the southeastern portion of the study area

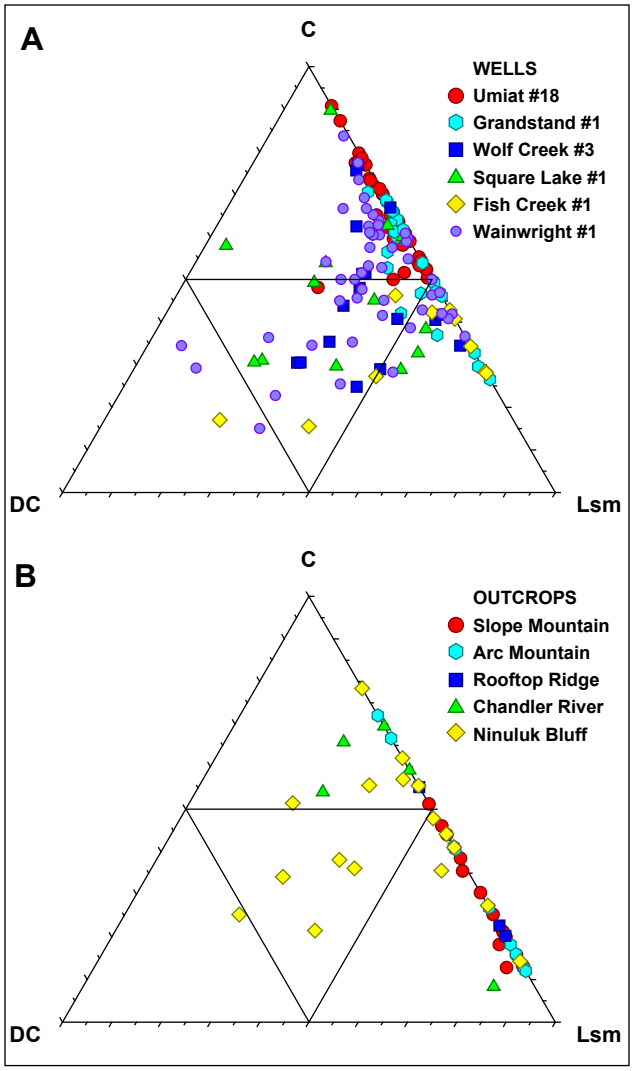

Figure 10. Chert (C) – Detrital Carbonate (DC) – Argillaceous Sedimentary/Metasedimentary Lithics (Lsm) ternary diagram detailing provenance implications for Nanushuk sandstone. The data were obtained via the traditional point-counting method in which phaneritic rock fragments are classified by their lithology (for example, granite, diorite, gabbro, gneiss). (**A**) Diagram for six NPRA wells. Nanushuk sandstone in the southeastern wells (Grandstand 1 and Umiat 18) contains little detrital carbonate while to the northwest (Wolf Creek 3, Square Lake 1, Fish Creek 1, and Wainwright 1) it contains a significant, and somewhat variable, quantity. (**B**) Diagram for five outcrop sections from the central North Slope. Nanushuk sandstone from the southeastern outcrops (Slope Mountain, Arc Mountain, and Rooftop Ridge) contains little to no detrital carbonate, while that to the northwest (Chandler River and Ninuluk Bluffs) contains significantly more. The trend seen in outcrop parallels the subsurface trend.

(Slope Mountain, Arc Mountain, and Rooftop Ridge) contains little to no (range 0–1 percent bulk rock, mean 0.07 percent) detrital carbonate (figs. 10B, 11B), while sandstone from the northwest (Chandler River and Ninuluk Bluff) contains a significantly greater quantity (range 0–17 percent bulk rock, mean 4.6 percent).

Potential sources of detrital carbonate in Nanushuk sandstone include the Mississippian-Pennsylvanian Lisburne Group in the Endicott Mountains allochthon and in uplifts in the Lisburne Hills/Herald arch area that contain abundant carbonate rocks, including thick dolomite sections. In addition, limestones of the Baird Group, which is present in the Kelly River, Ipnavik, and Nuka Ridge allochthons in the western Brooks Range, also are potential sources of detrital limestone in Nanushuk sandstone. It seems probable that these grains were derived from allochthons in the western Brooks Range and uplifts in the Herald arch. It is uncertain if detrital carbonate could survive long-distance fluvial transport from sources in eastern Siberia, a present-day distance of approximately 1,000 km.

RESERVOIR QUALITY

General Considerations

Reservoir quality (porosity, permeability) of the Nanushuk siltstone and sandstone from the 5 wells in this study (fig. 12A) varies widely from very poor (5 percent porosity, 0.002 md permeability; Umiat 18, 741 ft measured depth) to excellent (31 percent porosity, 4110 md permeability; Fish Creek 1, 2970 ft measured depth). For the Umiat 18 samples, as noted above, variation in reservoir quality, with exception of cemented samples, is largely controlled by depositional energy as signaled by grain size. It is presumed that variations in reservoir quality within Fish Creek 1, Square Lake 1, Grandstand 1, and Wolf Creek 3 are also controlled largely by depositional energy, although grain-size data are insufficient to affirm

that relationship. Porosity-permeability data for the regional Nanushuk samples plot in two distinct groups: one that mimics the trend exhibited by the Umiat 18, Grandstand 1, and Wolf Creek 3 samples (red dashed oval in fig. 12A), and a second parallel trend, represented by the Fish Creek 1 (single data point) and Wainwright 1 samples, that has higher porosity values for a given permeability (green dashed oval in fig. 12A). The disparity in reservoir quality between the two groups is interpreted to result from differences in burial, specifically the maximum burial the rocks experienced (fig. 12B). The high-porosity group consists almost exclusively of samples with a Dmax of less than 7,000 ft, while samples from the low-porosity group consistently have Dmax greater than 7,000 ft (fig. 12B). The Dmax value of 7,000 ft was determined empirically by analyzing the entire set of available data and testing which Dmax value provided the best discrimination between the two trends.

Differences in reservoir quality based on modal data are graphically illustrated in a PFC (Porosity-Framework-Cement) diagram (fig. 13); a technique originally proposed by Franks and Lee

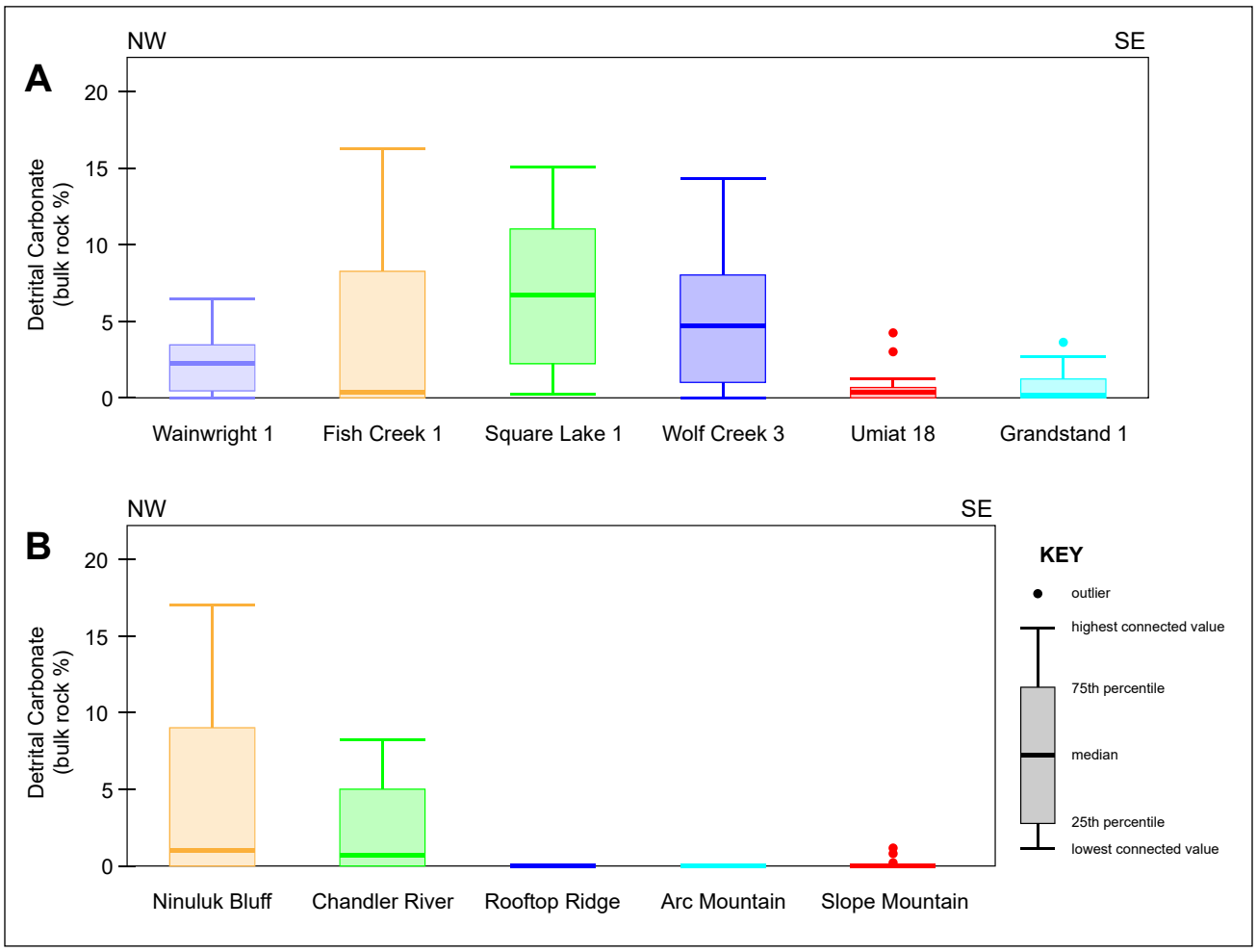

Figure 11. Boxplots for detrital carbonate (in bulk rock percent). The rectangular box represents the range between the 25th and 75th percentiles of the values; the heavy line within the box is the median value. The upper and lower whiskers represent the ranges of the highest connected and lowest connect values, respectively. Dots above the upper whiskers are outlier values. The statistics are calculated by Data Desk (Velleman, 1998). **A**. Boxplots for six NPRA wells; one extreme outlier for the Fish Creek 1 well (value of 28 percent bulk rock) was excluded from the figure for the sake of compactness but was included in statistical calculations. **B**. Boxplots for five outcrop sections from the central North Slope. Both the subsurface and outcrop data exhibit detrital carbonate amounts, and to a lesser extent variability, that increase from southeast to northwest.

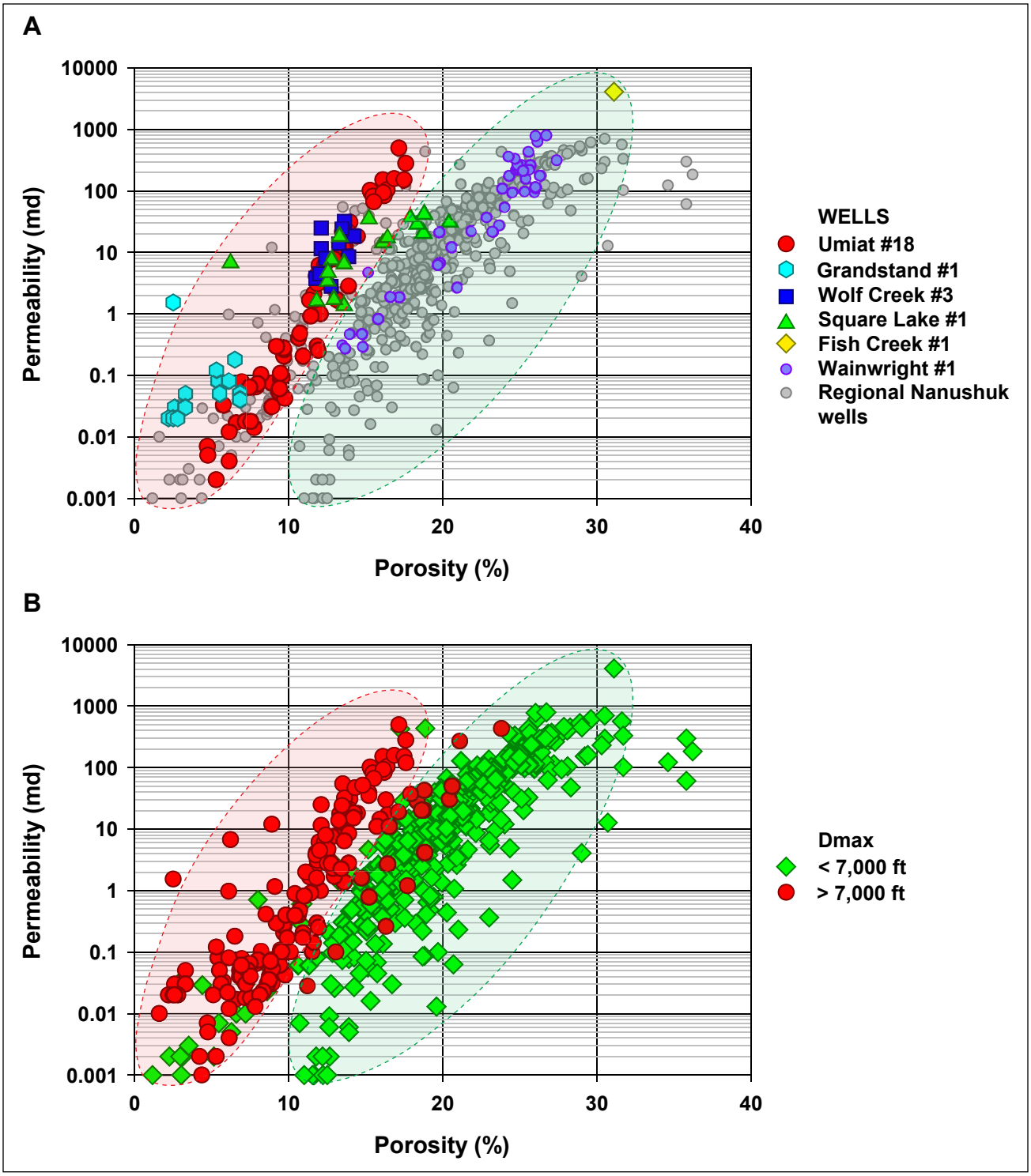

Figure 12. Porosity–permeability cross plot showing reservoir quality of Nanushuk sandstone from six NPRA wells and associated regional samples. Two parallel trends are evident: One for rocks with higher porosity (green dashed oval) and the other for rocks with lower porosity (red dashed oval). **A**. Samples are coded by well. Sandstone from Fish Creek 1 and Wainwright 1 is characteristic of the better reservoir-quality rock that has not been deeply buried, while sandstone from Square Lake 1, Grandstand 1, Wolf Creek 3, and Umiat 18 is characteristic of the poorer reservoir-quality rock subjected to moderate to deep burial. **B**. Same plot shown in A, with samples coded by Dmax. Most of the samples within the green oval have a Dmax of less than 7,000 ft, while those within the red oval have a Dmax greater than 7,000 ft. This supports the interpretation that the two parallel trends result from differences in Dmax.

(1994). The Fish Creek 1 samples fall largely into the "compacted reservoir" area of the diagram while the Square Lake 1, Grandstand 1, and Wolf Creek 3 samples largely plot in the "compacted non-reservoir" field. The Umiat 18 samples lie in both the "compacted reservoir" and "compacted non-reservoir" fields. The regional Nanushuk samples are largely confined to the "compacted reservoir" and "compacted non-reservoir" fields, although several plot in the "preserved reservoir" portion of the diagram. A limited number of the Square Lake 1 and regional samples lie in the "cemented non-reservoir" field attesting that porosity is largely destroyed by compaction. This is confirmed by a cross plot of compactional porosity loss (COPL; Lundegard, 1992) versus cementational porosity loss (CEPL) which shows a similar relationship (fig. 14). The vast majority of Fish Creek 1, Square Lake 1, Grandstand 1, Wolf Creek 3, Umiat 18, and regional Nanushuk samples have COPL values of 25–45 percent with corresponding CEPL values of less than 10 percent confirming that, for most samples, mechanical compaction plays a much larger role in porosity destruction than cementation.

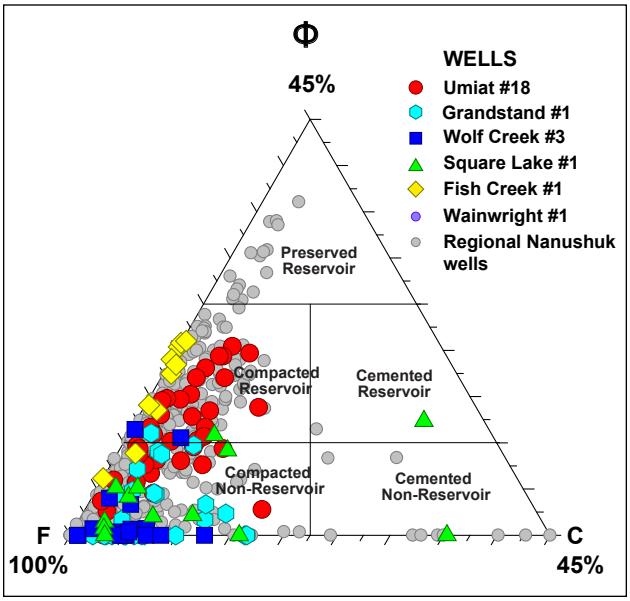

Figure 13. Porosity (Φ) – Framework Grains (F) – Cement (C) ternary diagram showing reservoir quality of six NPRA wells and regional Nanushuk siltstone and sandstone. Wolf Creek 3, Square Lake 1, and many of the Uniat 18 samples plot in the "compacted non-reservoir" area of the diagram while most of the Fish Creek 1 and the remaining Umiat 18 samples plot in the "compacted reservoir" field. The regional Nanushuk samples plot mainly in the "compacted non-reservoir" and "compacted reservoir" fields, although a few plot in the "preserved reservoir" and "cemented non-reservoir" fields. This confirms that porosity loss in Nanushuk sandstone is dominantly through compaction. Diagram modified from Franks and Lee (1994); used with permission.

Forward-Looking Predictions

In sedimentary basins where calibration datasets are available, regression analysis has proved an effective method for predicting reservoir quality (Scherer, 1987; Bloch, 1991; Byrnes and Wilson, 1991; Bloch and Helmold, 1995). This is especially true for sandstone that contains less than 10 percent cement or in which only small volumes of sandstone are highly cemented. In the latter case, inclusion of highly cemented samples in the regression analyses can yield overly pessimistic forecasts. One approach is to exclude highly cemented samples from the input data, thereby yielding predictions for only uncemented or moderately cemented sandstone. This is a viable approach when the highly cemented samples occur in thin zones (e.g., carbonate streaks) or as isolated concretions. The rationale from an exploration perspective, is that these thin, highly cemented zones are not representative of the overall reservoir and their presence will have little impact on whether the host sandstone can produce hydrocarbons. Previous studies have shown that Brookian sandstones of the North Slope, in which compaction is the dominant mechanism of porosity destruction, are good candidates for regression analysis (Smosna, 1989). This is particularly true for the Cretaceous Torok and Nanushuk Formations, and slightly less so for the Seabee Formation.

Previous work on Torok and Seabee reservoirs has established that reservoir quality expected in a prospect can be forecast reasonably well by utilizing Dmax as the predictor (independent) variable and porosity and permeability as the response (dependent) variables in regression analyses (Helmold and others, 2006). In partially exhumed sedimentary basins, Dmax is calculated by adding the amount of

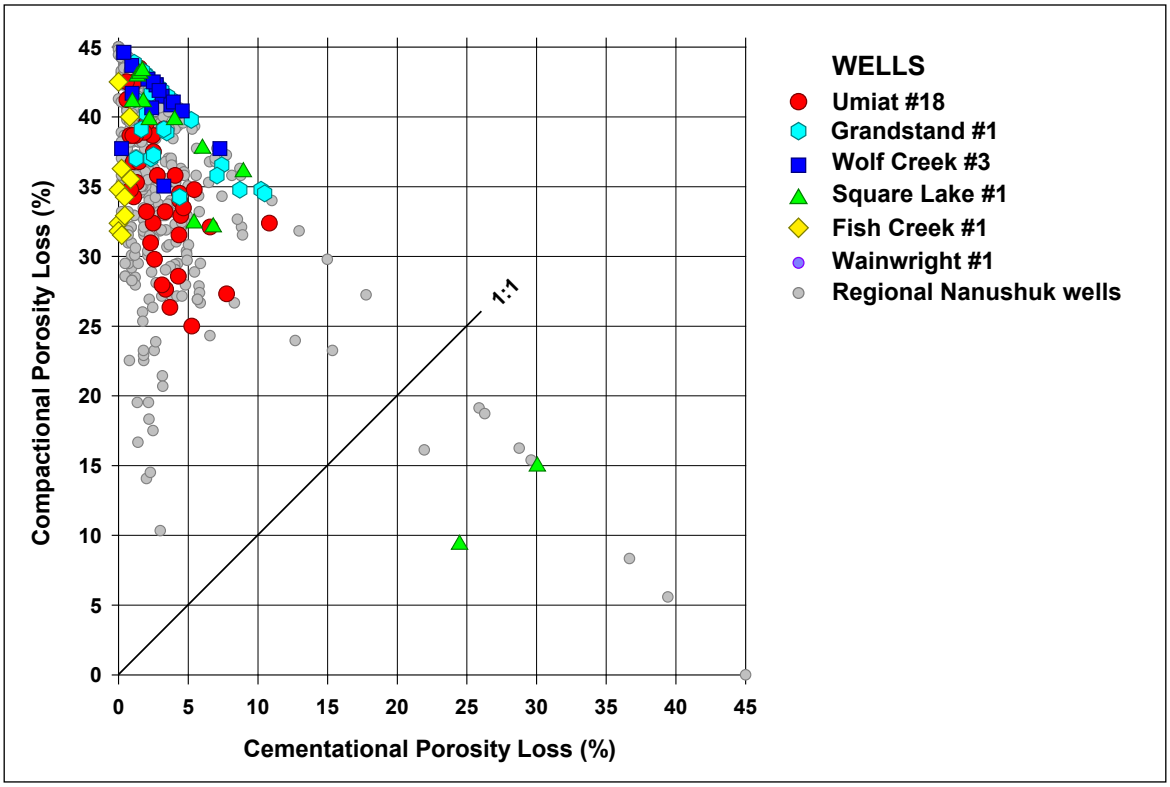

Figure 14. Cross plot of compactional porosity loss versus cementational porosity loss for six NPRA wells and regional Nanushuk siltstone and sandstone. Samples with cementational porosity loss greater than 45 percent are arbitrarily set to the assumed maximum depositional intergranular volume of 45 percent. The diagonal line (1:1) represents equal porosity loss by compaction and cementation. Porosity loss in most samples was largely through compaction. Diagram modified from Lundegard (1992).

denuded section to the current burial depth. Burns and others (2005) utilized sonic-porosity well logs to estimate the amount of sedimentary section eroded on the North Slope, thereby enabling the value of Dmax to be estimated for any exploration well. A contour map of eroded section for the central North Slope displays a generally uniform increase in the thickness of eroded section, and hence Dmax, from the Barrow Arch in the north to the Brooks Range deformation front in the south (fig. 15). Fish Creek 1 is located along the northern Alaska coastline where the thickness of eroded section is estimated at 1,103 ft (fig. 15, modified from Burns and others, 2005). That amount added to the current burial depths of Fish Creek samples, yields maximum depths of burial (Dmax) ranging from 4,074 to 4,136 ft (figs. 15, 16). Similarly, Wainwright 1 experienced 2,762 ft of denudation, with corresponding Dmax values of 2,944 to 4,263 ft (figs. 15, 16; Helmold, 2016). Most geologists consider burial less of than 5,000 ft as shallow to moderate. In contrast, Grandstand 1, Wolf Creek 3, and Umiat 18 are located 80 to 100 miles south of the Beaufort Sea where estimates of removed overburden are much greater (fig. 15, table 1). Specifically, at Umiat 18 the amount of denudation is estimated at 6,485 ft (fig. 15, modified from Burns and others, 2005), resulting in Dmax values ranging from 7,199 to 7,496 ft (figs. 15, 16). Grandstand 1 and Wolf Creek 3 are more extreme examples; the thickness of eroded section at Grandstand 1 is estimated at 8,084 ft (fig. 15, modified from Burns and others, 2005), resulting in Dmax values ranging from 8,326 to 10,596 ft (figs. 15, 16). For Wolf Creek 3 the amount of denudation is estimated at 7,191 ft, yielding Dmax values ranging from 8,724 to 10,711 ft (figs. 15, 16). Many of the southern wells in the regional dataset have similar burial histories with maximum depths of burial

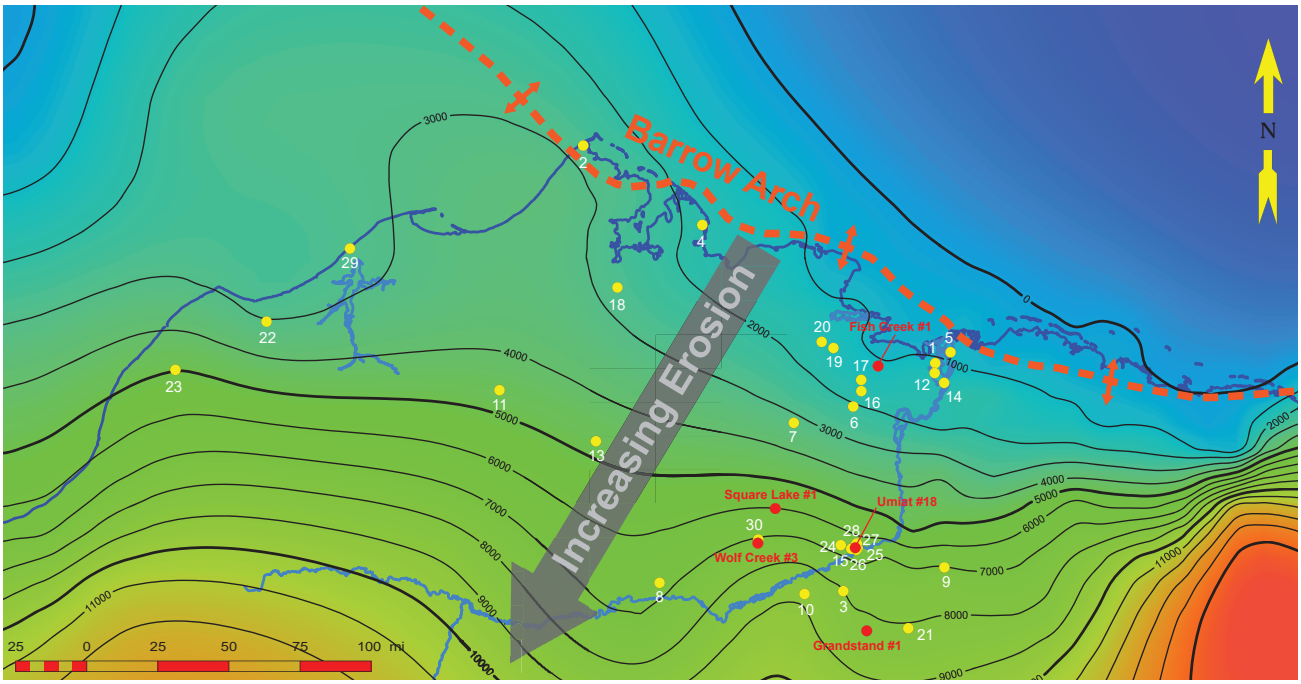

Figure 15. Contoured map of the central north slope of Alaska showing estimates of the thickness of Brookian strata removed by erosion (in feet). Red circles show the location of the five NPRA wells in this study; yellow circles show locations of thirty (30) wells for which petrographic data are available for Nanushuk sandstone (see table 1 for list). The large arrow shows the regional trend of increasing amounts of erosion to the south. Contours were generated from the data of Burns and others (2005) using GeoAtlas—the mapping module of GeoGraphix.

approaching 10,000 ft (figs. 15, 16); such values are traditionally considered deep burial.

Using available data, two sets of linear regression models for porosity-Dmax and permeability-Dmax relationships were developed for Nanushuk sandstone. Samples known or suspected to have greater than 10 percent carbonate cement were excluded from the analyses. One model (full-dataset model) uses all available porosity, permeability, and Dmax data (fig. 16, table 3), while the other (mean-value model) uses mean values of porosity, permeability, and Dmax calculated for each well (fig. 17). The two models give similar results, although with differing degrees of complexity. The mean-value analysis produces a plot (fig. 17) in which data points representing individual wells better conform to the regression line thereby yielding a higher correlation coefficient (r = -0.82 for porosity). Although this plot is more visually appealing, it hides the true intricacy of the data. Analysis of the full dataset (fig. 16) yields a lower correlation coefficient (r = -0.79 for porosity) but allows for a better understanding of the factors controlling reservoir quality. For any conventional core in each well, individual samples have similar values of Dmax (within 30 to 60 ft—the standard length of conventional core barrels) and form nearly vertical lines in the plot (fig. 16). Two factors are thought to govern the reservoir quality of Brookian sandstone: depositional environment, which is considered a local control; and depth of burial, which is deemed a regional factor. The large spread in porosity and permeability for any given value of Dmax (i.e., any given core) illustrates the primary (local) control depositional environment has on reservoir quality. This realization is lost in the mean-value model. Both analyses illustrate the secondary (regional) control that burial history has on reservoir quality. The porosity-Dmax plot yields a more tightly constrained relationship (higher correlation coefficient) than the permeability-Dmax plot in both the mean-value and full-dataset models. This is to be expected

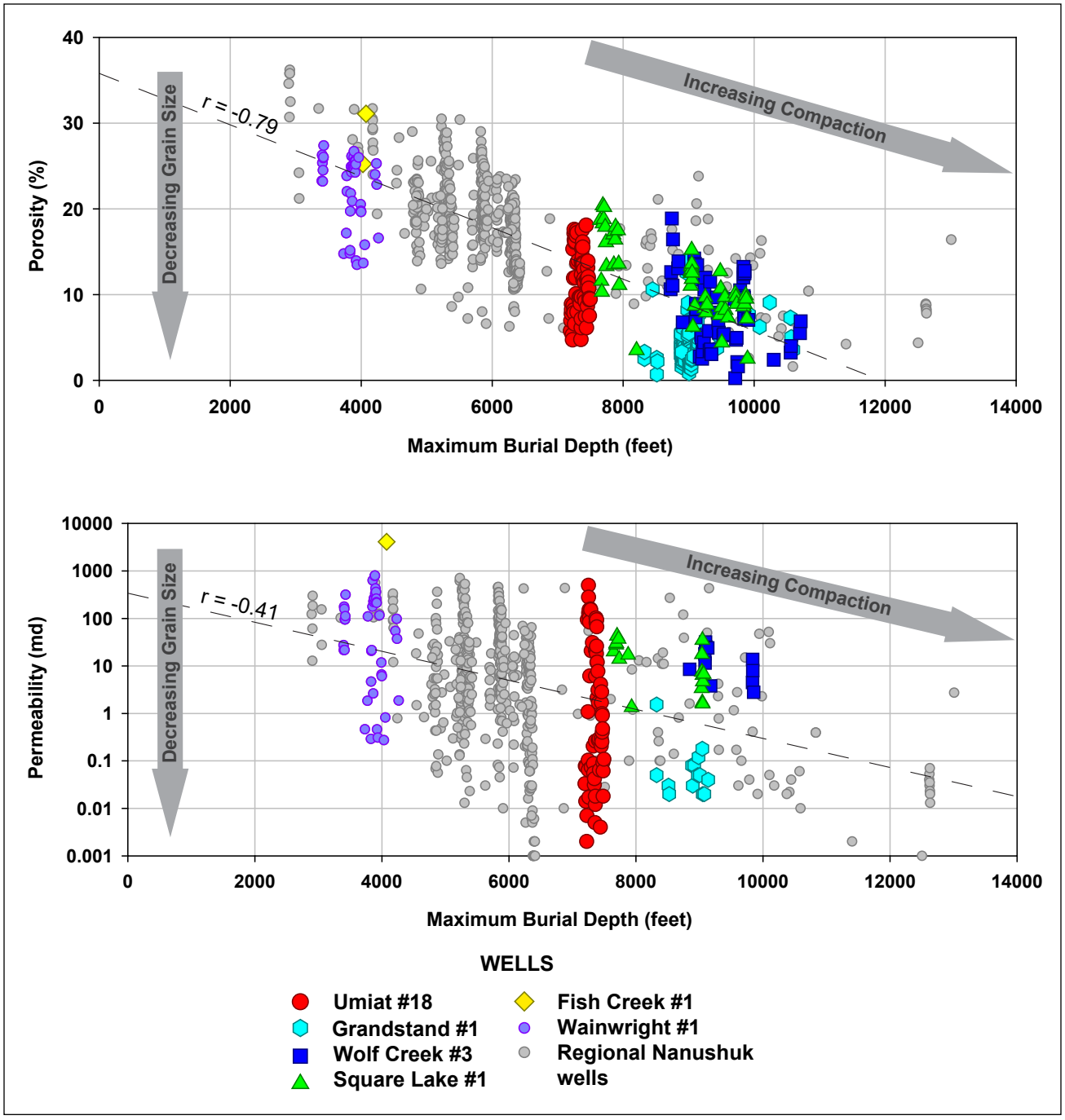

Figure 16. Cross plots of reservoir quality versus maximum burial depth (Dmax) for six NPRA wells and regional Nanushuk samples. All available data were plotted (compare with fig. 17) except for samples with > 10 percent carbonate cement. The arrows depict the two major controls on Nanushuk reservoir quality: depositional environment (grain size as proxy) and compaction. At any given value of Dmax, reservoir quality is largely controlled by depositional energy as signaled by grain size. At the regional scale, compaction has a significant effect on reservoir quality. **A**. Porosity versus Dmax plot; Wainwright 1 samples are indicative of shallow samples (~ 4,000 ft Dmax) while those from Wolf Creek 3 are representative of deeply buried rocks (> 9,000 ft Dmax). **B**. Permeability versus Dmax plot. Permeability data have a larger standard deviation than porosity data.

Table 3. Linear regression models to predict porosity and permeability of Nanushuk sandstone from maximum burial depth (Dmax). The models use all available porosity, permeability, and Dmax data; samples with greater than 10% carbonate cement are excluded (fig. 16). When applied to pre-drill predictions, an estimate of the maximum burial depth of the reservoir yields predictions for the mean values of core porosity and permeability. Estimates of the range of individual values are given by the mean ± 1 σ. Coefficient of porosity intercept = 35.7982, coefficient of porosity slope = -0.00301337, coefficient of log(permeability) intercept = 2.53536, coefficient of log(permeability) slope = -0.000308174.

All Data						
	Porosity Regression			Permeability Regression		
Dmax	Porosity	Porosity - 1σ	Porosity + 1σ	Permeability	Permeability - 1σ	Permeability + 1σ
1,000	32.8	25.5	40.1	168.728	8.186	3477.891
2,000	29.8	22.5	37.1	82.987	4.026	1710.575
3,000	26.8	19.5	34.1	40.817	1.980	841.333
4,000	23.7	16.4	31.0	20.075	0.974	413.803
5,000	20.7	13.4	28.0	9.874	0.479	203.526
6,000	17.7	10.4	25.0	4.856	0.236	100.103
7,000	14.7	7.4	22.0	2.389	0.116	49.235
8,000	11.7	4.4	19.0	1.175	0.057	24.216
9,000	8.7	1.4	16.0	0.578	0.028	11.910
10,000	5.7	0.0	13.0	0.284	0.014	5.858
11,000	2.7	0.0	9.9	0.140	0.007	2.881
12,000	0.0	0.0	7.3	0.069	0.003	1.417
13,000	0.0	0.0	7.3	0.034	0.002	0.697
14,000	0.0	0.0	7.3	0.017	0.001	0.343

given the large range of permeability in sandstone. The predicted values of porosity and permeability derived from the regression models are essentially mean values for a given value of Dmax. Estimates of the range in individual values of porosity and permeability are obtained by adding (high end of range) and subtracting (low end of range) the value of one sigma of the entire population from the mean (table 3). When using these regression models to forecast reservoir quality prior to drilling, it is important to keep in mind the implied assumptions: 1) petrology of the target sandstone is comparable to that in the modeled wells, and 2) the depositional environments in the target well are akin to those represented in the modeled wells. The greatest expected source of error in the forecasts lies in the possible occurrence of depositional facies that were not present in the modeled wells. Similar regression analyses for Torok and Seabee sandstones have proven useful in predicting reservoir quality prior to drilling (Helmold and others, 2006) and have led to a better understanding of the regional distribution of reservoir sandstone on the North Slope (table 4).

Musings on the Big Picture

Reservoir quality of Nanushuk sandstone is largely controlled by two separate and independent processes: depositional environment, which establishes a local control, and compaction, which constitutes a regional control (fig. 16). Many facets of sediment deposition influence reservoir quality, such as grain size, sorting, bioturbation, laminations, sedimentary structures, and clay content to name a few. Given the disparate and incomplete datasets used in this and other regional studies, grain size emerges as a useful parameter that is often measured during sedimentologic and petrographic studies. While not a direct analog, grain size can be used as a proxy for depositional environment, more specifically as a measure of depositional energy. At the local-con-

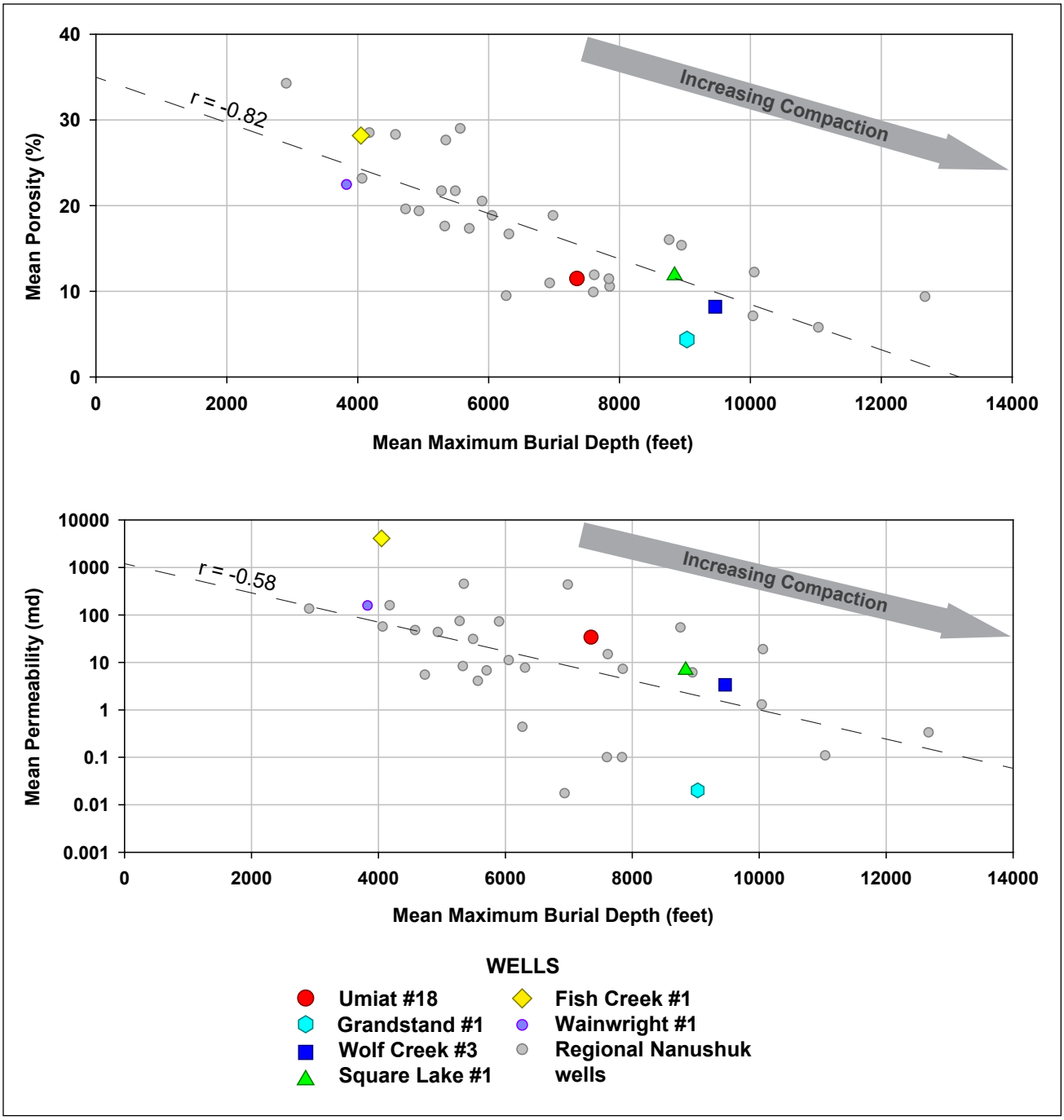

Figure 17. Cross plots of reservoir quality (as mean porosity and mean permeability) versus mean maximum burial depth (Dmax) for six NPRA wells and regional Nanushuk samples. Mean values are plotted by well (compare with fig. 16); samples with > 10 percent carbonate cement were excluded from the means. The arrow depicts the regional control compaction has on reservoir quality; the local control of depositional environment, as indicated by grain size, is not evident from plots of mean values. Correlation coefficients are greater than for plots incorporating all the data (fig. 16), but complexity of the data is hidden. **A**. Porosity versus Dmax plot; Wainwright 1 is indicative of shallow samples (~ 4,000 ft Dmax) while Wolf Creek 3 is representative of deeply buried rocks (> 9,000 ft Dmax). **B**. Permeability versus Dmax plot.

Table 4. Predictions of reservoir quality of Torok and Seabee sandstone from maximum burial depth (Dmax). Regression model uses all available data; samples with >10 percent carbonate cement are excluded. Predicted values are mean porosity and permeability. Dmax values < 8,000 ft (green zone) yield productive reservoirs, Dmax values of 8,000–9,000 ft (yellow zone) yield marginal reservoirs, sandstone with >9,000 ft Dmax (red zone) are non-productive. Estimates of the range of individual values are given by the mean ± 1 σ. Coefficient of porosity intercept = 37.6734, coefficient of porosity slope = -0.00274949, coefficient of log(permeability) intercept = 3.29548, coefficient of log(permeability) slope = -0.000431553.

			Mean Porosity				Mean Permeability			
Well	Formation	Dmax	$Ø_{predicted}$	$Ø_{actual}$	$Ø_{predicted \pm 1\sigma}$	$Ø_{actual \pm 1\sigma}$	$K_{predicted}$	K_{actual}	$K_{predicted \pm 1\sigma}$	$K_{actual \pm 1\sigma}$
Kalubik 2	Torok	5,814	21.7	18.4	15.8–27.5	15.0–21.9	6.12	8.08	0.39–95.3	0.0–25.6
Kalubik 1	Torok	5,969	21.3	20.0	15.4–27.1	17.5–22.5	5.24	13.97	0.34–81.7	0.0–28.2
Bergschrund 1	Torok	7,002	18.4	13.9	12.6–24.3	4.0–9.9	1.88	3.00	0.12–29.3	0.0–6.9
Tarn 2N-313	Seabee	7,198	17.9	20.5	12.0–23.7	16.9–24.2	1.55	37.11	0.10–24.1	0.0–105.2
Tarn 3	Seabee	7,259	17.7	15.2	11.9–23.6	12.2–18.3	1.45	1.49	0.09–22.7	0.0–5.3
Tarn 2	Seabee	7,417	17.3	16.3	11.4–23.1	12.7–19.9	1.24	3.43	0.08–19.4	0.0–10.3
Tarn 4	Seabee	7,502	17.0	15.6	11.2–22.9	11.0–20.2	1.14	1.65	0.07–17.8	0.0–4.7
Aklaq 2	Torok	7,542	16.9	13.3	11.1–22.8	9.4–17.3	1.10	1.90	0.07–17.1	0.4–3.5
Cirque 3	Seabee	7,638	16.7	14.8	10.8–22.5	11.9–17.7	1.00	1.79	0.06–15.6	0.0–2.6
Meltwater North 2A	Seabee	7,683	16.5	16.9	10.7–22.4	12.2–21.7	0.95	6.94	0.06–14.9	0.0–17.7
Nanuk 1	Torok	7,691	16.5	15.5	10.7–22.4	13.8–17.2	0.95	2.08	0.06–14.8	0.0–4.3
Nanuk 2	Torok	7,754	16.4	15.8	10.5–22.2	13.7–17.9	0.89	3.70	0.06–13.9	0.0–7.9
Meltwater North 2	Seabee	7,839	16.1	13.1	10.3–22.0	9.6–16.6	0.82	1.99	0.05–12.7	0.0–8.7
Bermuda 1	Torok	7,860	16.1	20.3	10.2–21.9	18.3–22.3	0.80	11.83	0.05–12.5	0.7–22.9
Meltwater North 1	Seabee	7,864	16.1	16.7	10.2–21.9	12.5–20.9	0.80	6.72	0.05–12.4	0.0–19.5
Trailblazer A1	Torok	8,119	15.4	8.2	9.5–21.2	7.0–9.3	0.62	0.02	0.04–9.6	0.0–0.0
Aklaq 2	Torok	8,261	15.0	11.7	9.1–20.8	8.3–15.1	0.54	0.30	0.03–8.4	0.0–0.8
Trailblazer H1	Torok	8,293	14.9	8.4	9.0–20.7	7.0–9.9	0.52	0.04	0.03–8.1	0.0–0.1
Atlas 1	Torok	8,320	14.8	13.9	8.9–20.6	12.2–15.7	0.51	0.45	0.03–7.9	0.0–1.0
Aklaq 2	Torok	8,637	13.9	11.6	8.1–19.8	9.1–14.0	0.37	0.20	0.02–5.8	0.0–0.3
Kokoda 1	Torok	8,666	13.8	10.0	8.0–19.7	8.8–11.2	0.36	0.08	0.02–5.6	0.0–0.1
Aklaq 2	Torok	8,913	13.2	11.4	7.3–19.0	8.5–14.3	0.28	0.20	0.02–4.4	0.0–0.3
Aklaq 2	Torok	9,069	12.7	11.7	6.9–18.6	10.7–12.7	0.24	0.10	0.02–3.8	0.1–0.2
Meltwater South 1	Seabee	9,086	12.7	11.5	6.8–18.5	9.5–13.5	0.24	0.35	0.02–3.7	0.0–1.6
Cronus 1	Torok	9,200	12.4	10.0	6.5–18.2	–	0.21	–	0.01–3.3	–
Aklaq 2	Torok	9,302	12.1	5.7	6.2–17.9	5.3–6.1	0.19	0.10	0.01–3.0	0.0–0.1
Caribou 1	Torok	9,768	10.8	5.7	5.0–16.7	2.7–8.8	0.12	0.01	0.01–1.9	0.0–0.03
Hunter A	Torok	9,781	10.8	9.3	4.9–16.6	7.8–10.7	0.12	0.08	0.01–1.8	0.0–0.19
Caribou 1	Torok	10,074	10.0	8.9	4.1–15.8	6.5–11.3	0.09	0.07	0.01–1.4	0.02–0.12
Caribou 1	Torok	10,288	9.4	9.1	3.5–15.2	7.5–10.8	0.07	0.04	0.00–1.1	0.02–0.05
Grizzly 1	Torok	10,820	7.9	5.9	2.1–13.8	4.1–7.7	0.04	–	0.00–0.7	–
Heavenly 1	Torok	11,995	4.7	9.9	0.0–10.5	8.0–11.8	0.01	–	0.00–0.2	–

trol level, porosity and permeability are largely a function of depositional energy of the depositing currents which can be estimated by grain size of the detritus. Higher-energy depositional environments are characterized by coarser-grained detritus which typically have better reservoir quality. Conversely, lower-energy depositional environments consist of finer-grained detritus that exhibit poor reservoir quality. From a regional-control perspective porosity and permeability of Brookian sandstone is reduced as the rock, regardless of grain size or depositional environment, is buried to greater depths. Hence, on the North Slope there is a decrease in overall reservoir quality from north to south corresponding to progressively greater uplift, denudation, and maximum burial. Sandstone that has not seen significant burial (vicinity of the Beaufort Sea) is characterized by large spreads in porosity and permeability. This variability is controlled almost exclusively by depositional energy as signaled by grain size. In contrast, sandstone that has undergone deep burial (vicinity of Brooks Range deformation front) displays narrower ranges in porosity and permeability; reservoir quality being controlled by both depositional energy and compaction (figs. 16, 17).

Another important conclusion is that provenance does not exert a significant control on reservoir quality for the majority of Nanushuk samples examined in this study. Despite the variability in chert (related to grain size) and detrital carbonate (related to aerial distribution) content noted above, most samples have a somewhat uniform composition characterized by an abundance of argillaceous sedimentary and metasedimentary rock fragments. These lithic fragments are highly susceptible to ductile grain deformation; hence burial history, particularly maximum burial depth, of the sandstone is a critical factor in determining its reservoir potential. Recent work (Helmold and others, 2021) suggests there is more variability in Nanushuk composition than noted in the samples of this report. Nanushuk sandstone having a more quartzose composition and containing silica cement in the form of quartz overgrowths has been reported from outcrop samples collected from measured stratigraphic sections in the central North Slope (Helmold and others, 2021). The presence of significant overgrowths relegates this sandstone to a distinctly different diagenetic pathway than the more argillaceous lithic-rich variants. Additional work is needed to pinpoint similar quartzose sandstone in the subsurface.

Based on analysis of datasets in this report, it is possible to make general conclusions concerning the relationships between porosity, permeability, and maximum burial depth for Brookian sandstone of the North Slope. Uncemented and lightly cemented sandstone that was subjected to limited burial should show a wide range in porosity and permeability with reservoir quality largely controlled by depositional energy as indicated by grain size, sorting, mica and detrital matrix content, and lateral continuity of clay and mudstone laminations. Porosity values approaching 45 percent (presumed depositional porosity) can be expected for coarser-grained detritus with little mica, clay, or laminations of finer-grained sediment. Finer-grained, more mica- and clay-rich, or laminated sandstone should have lower porosity, potentially approaching 10–15 percent (fig. 18). As sandstone is subjected to increased burial, the overall variability of porosity and permeability is expected to decrease. Deep burial (>10,000 ft) results in significant mechanical compaction that reduces both the mean value and range of porosity and permeability, with porosities typically less than 10 percent. The theoretical data cloud in a porosity-Dmax cross plot for sandstone will tend to form a right trapezoid, with a longer base at lower burial depth and a shorter base at greater burial (fig. 18). (Note on terminology: a right trapezoid is a convex quadrilateral with one pair of parallel sides and two adjacent right angles. The parallel sides are termed the bases of the trapezoid, while the non-parallel sides are called the legs of the trapezoid.) The theoretical data cloud in a permeability-Dmax cross plot should show a similar shape. The actual porosity-Dmax data for Nanushuk sandstone presented in this report (fig. 16A) fall short of the idealized trend due to the dearth of samples with minimal burial (low Dmax). It is anticipated

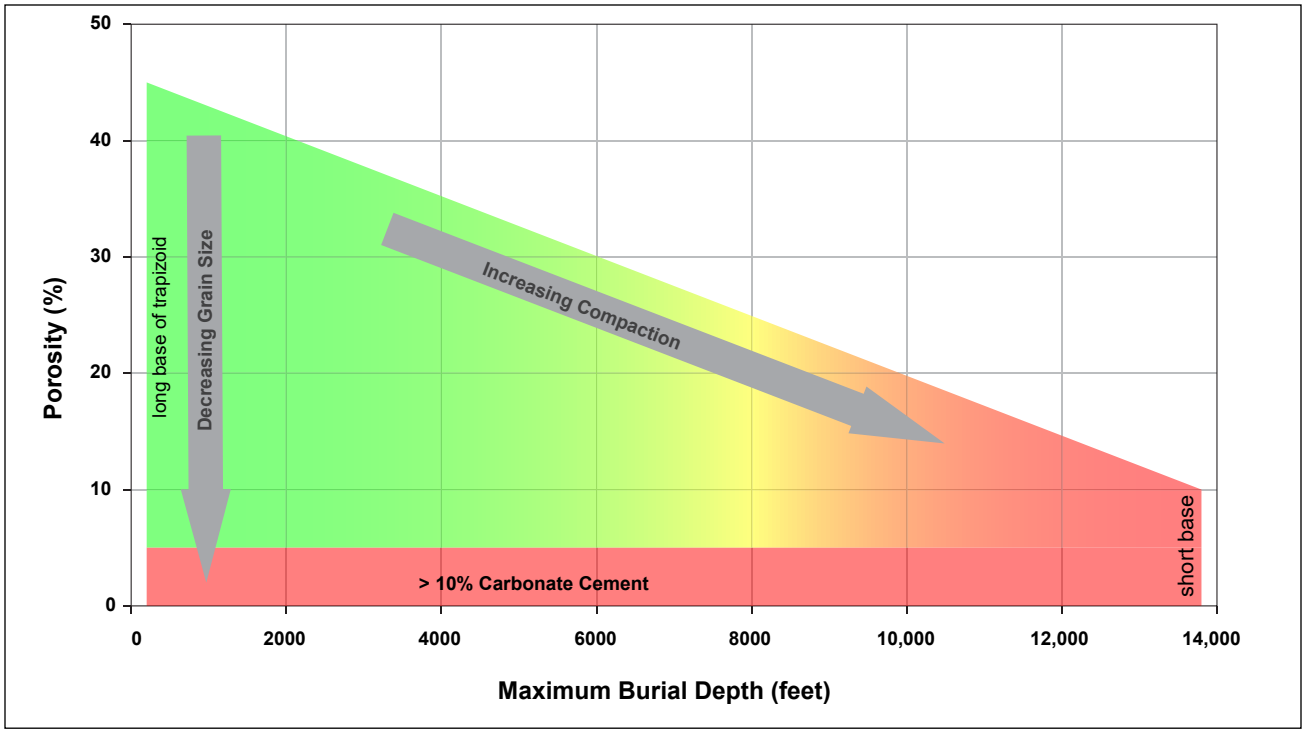

Figure 18. Theoretical plot of porosity versus maximum burial depth (Dmax) showing the idealized right trapezoid shape of the data cloud, with a longer base at lower burial depth and a shorter base at greater burial. Sandstone with >10 percent carbonate cement occurs as a narrow band with low porosity along the right-angle leg of the trapezoid. The green–yellow–red color shading shows the relative extent of reservoir quality; a value of ~8,000 ft Dmax marks the approximate boundary between productive and non-productive Brookian reservoirs. The arrows signify local (depositional energy as indicated by grain size) versus regional (compaction) controls on reservoir quality. A theoretical plot of permeability versus Dmax should have a similar shape.

the cloud from a larger dataset would more nearly resemble the theoretical quadrilateral.

The presence of significant cement, particularly diagenetically early cement, alters the appearance of the cross plot. Sandstone with appreciable cement (typically > 10 percent) will have poor reservoir quality regardless of its burial history and will plot as a narrow band with low porosity and permeability along the right-angle leg of the trapezoid (fig. 18).

Similar generalizations can be made for theoretical porosity-permeability cross plots of sandstone in the basin. Regardless of burial, the porosity-permeability trend for sandstone in any given well should plot as a diagonal line (fig. 19). Sandstone subjected to shallow burial will plot on the right-hand portion of the diagram (higher porosity values), while more deeply buried sandstone will plot farther to the left (lower porosity values). Both the local control of depositional environment as signaled by grain size and the regional control of compaction can be delineated on the plots.

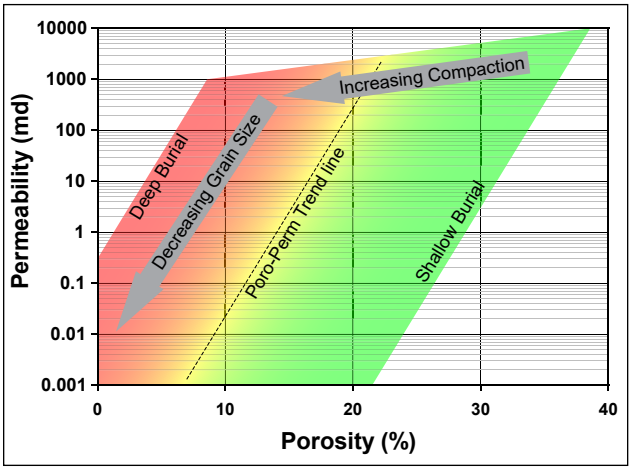

Figure 19. Theoretical plot of porosity versus permeability showing idealized parallel trends exhibited by Brookian sandstone subjected to shallow (green zone), moderate (yellow zone), and deep burial (red zone). The arrows signify local (depositional energy as indicated by grain size) versus regional (compaction) controls on reservoir quality.

ACKNOWLEDGMENTS

Funding for this work was provided by the State of Alaska. The Alaska Geologic Materials Center provided thin sections from the Fish Creek 1, Square Lake 1, Grandstand 1, and Wolf Creek 3 wells; the assistance of Kurt Johnson and Jean Riordan is greatly appreciated. Corri Feige, DNR Commissioner, was instrumental in gaining access to material and data from the Umiat 18 core. Linc Energy granted access to thin sections and routine core analyses from the core. Leonard Sojka, Malamute Energy, Inc., facilitated the loan of this material to DGGS/DOG. Insightful formal reviews by Andrew Dewhurst, Colby VanDenburg, Nina T. Harun, Ellen Daley, and Astrid Makowtiz were helpful in improving the final report.

REFERENCES

Ahlbrandt, T.S., Huffman, A.C., Fox, J.E., and Pasternack, I., 1979, Depositional framework and reservoir-quality studies of selected Nanushuk Group outcrops, North Slope, Alaska, *in* Ahlbrandt, T.S., ed., Preliminary geologic, petrologic, and paleontologic results of the study of Nanushuk Group rocks, North Slope, Alaska: U.S. Geological Survey Circular 794, p.14–31.

Atkinson, C.D., McGowen, J.H., Bloch, S., Lundell, L.L., and Trumbly, P.N., 1990, Braidplain and deltaic reservoir, Prudhoe Bay Field, Alaska: *in* Barwis, J.H., McPherson, J.G., and Studlick, J.R.J., eds., Sandstone Petroleum Reservoirs, Springer-Verlag, p. 205–224.

Bartsch-Winkler, S., 1979, Textural and mineralogical study of some surface and subsurface sandstones from the Nanushuk Group, western North Slope, Alaska, *in* Ahlbrandt, T.S., ed., Preliminary geologic, petrologic, and paleontologic results of the study of Nanushuk Group rocks, North Slope, Alaska: U.S. Geological Survey Circular 794, p. 61–76.

———1985, Petrography of sandstones of the Nanushuk Group from four measured sections, central North Slope, Alaska, *in* Huffman, A.C., Jr., ed., Geology of the Nanushuk Group and related rocks, North Slope, Alaska: U.S. Geological Survey Bulletin 1614, p. 75–95.

Bartsch-Winkler, S., and Huffman, A.C., Jr., 1988, Sandstone petrography of the Nanushuk Group and Torok Formation, *in* Gryc, George, ed., Geology and exploration of the National Petroleum Reserve in Alaska, 1974 to 1982: U.S. Geological Survey Professional Paper 1399, p. 801–831.

Basu, A., Young, S.W., Suttner, L.J., James, W.C., and Mack, G.H., 1975, Re-evaluation of the use of undulatory extinction and polycrystallinity in detrital quartz for provenance interpretations: Journal of Sedimentary Petrology, v. 45, no. 4, p. 873–882.

Blatt, H., 1982, Sedimentary Petrology: New York, NY, W. H. Freeman and Company, 564 p.

Blatt, H., Middleton, G.V., and Murray, R., 1980, Origin of Sedimentary Rock (2nd edition): Englewood Cliffs, NJ, Prentice-Hall, 782 p.

Bloch, S., 1991, Empirical prediction of porosity and permeability in sandstone: American Association of Petroleum Geologist Bulletin, v. 75, no. 7, p. 1,145–1,160.

Bloch, S., and Helmold, K.P., 1995, Approaches to predicting reservoir quality in sandstones: Association of Petroleum Geologist Bulletin, v. 79, no. 1, p. 97–115.

Boggs, S., Jr., 2009, Petrology of Sedimentary Rocks (2nd edition): New York, NY, Cambridge University Press, 600 p.

Burns, W.M., Hayba, D.O., Rowan, E.L., and Houseknecht, D.W., 2005, Estimating the amount of eroded section in a partially exhumed basin from geophysical well logs: An example from the North Slope *in* Haeussler, P.J., and Galloway, J.P., eds., Studies by the U.S. Geological Survey in Alaska: U.S. Geological Survey Professional Paper 1732-D, p. 1–18.

Byrnes, A.P., and Wilson, M.D., 1991, Aspects of porosity prediction using multivariate linear regression [abs.]: American Association of Petroleum Geologist Bulletin, v. 75, p. 548.

Collins, F.R., 1959, Test Wells, Square Lake and Wolf Creek Areas Alaska: U.S. Geological Survey Professional Paper 305-H, p. 423–484.

Crowder, R.K., 1989, Deposition of the Fortress Mountain Formation, *in* Mull, C.G., and Adams, K.E., eds., Bedrock geology of the east-

ern Koyukuk basin, central Brooks Range, and east-central Arctic Slope along the Dalton Highway, Yukon River to Prudhoe Bay, Alaska, Volume 2: Alaska Division of Geological & Geophysical Surveys Guidebook 7-20, p. 293–301. http://doi.org/10.14509/24134

Decker, J.E., 1985, Sandstones modal analysis procedure: Alaska Division of Geological & Geophysical Surveys Public Data File 85-3, 38 p.

Decker, J.E., and Helmold, K.P., 1985, The effect of grain size on detrital modes: A test of the Gazzi-Dickinson point-counting method– Discussion: Journal of Sedimentary Petrology, v. 55, p. 618–620.

Decker, P.L., 2010, Brookian sequence stratigraphic framework of the northern Colville foreland basin, central North Slope, Alaska (poster and presentation): DNR Spring Technical Review Meeting, Anchorage, April 21–22, 2010: Alaska Division of Geological & Geophysical Surveys, 30 p., 1 sheet. http://doi.org/10.14509/21861

Folk, R.L., 1974, Petrology of sedimentary rocks: Hemphill Publishing Co., Austin, TX, 182 p.

Fox, J.E., 1979, A summary of reservoir characteristics of the Nanushuk Group, Umiat Test Well 11, National Petroleum Reserve in Alaska, *in* Ahlbrandt, T.S., ed., Preliminary geologic, petrologic, and paleontologic results of the study of Nanushuk Group rocks, North Slope, Alaska: U.S. Geological Survey Circular 794, p. 42–53.

Fox, J.E., Lambert, P.W., Pitman, J.K., and Wu, C.H., 1979, A study of reservoir characteristics of the Nanushuk and Colville Groups, Umiat Test Well 11, National Petroleum Reserve in Alaska: U.S. Geological Survey Circular 820, 47 p.

Franks, S.G., and Lee, M.K., 1994, Preliminary report on diagenesis of upper Cook Inlet sandstones: Atlantic Richfield Company report, 46 p.

Garrity, C.P., Houseknecht, D.W., Bird, K.J., Potter, C.J., Moore, T.E., Nelson, P.H., and Schenk, C.J., 2005, U.S. Geological Survey 2005 oil and gas resource assessment of the central North Slope, Alaska: play maps and results: U.S. Geological Survey Open-File Report 2005-1182, 25 p.

Gillis, R.J., Decker, P.L., Wartes, M.A., Loveland, A.M., and Hubbard, T.D., 2014, Geologic map of the south-central Sagavanirktok Quadrangle, North Slope, Alaska: Alaska Division of Geological & Geophysical Surveys Report of Investigation 2014-4, 24 p., 2 sheets, scale 1:63,360. http://doi.org/10.14509/29138

Gryc, George, 1988, Introduction and role of the U.S. Geological Survey, *in* Gryc, George, ed., Geology and exploration of the National Petroleum Reserve in Alaska, 1974 to 1982: U.S. Geological Survey Professional Paper 1399, p. 1–12.

Helmold, K.P., 2016, Sedimentary petrology and reservoir quality of Albian-Cenomanian Nanushuk Formation sandstones, USGS Wainwright #1 test well, western North Slope, Alaska, *in* LePain, D.L., ed., Stratigraphic and reservoir quality studies of continuous core from the Wainwright #1 coalbed methane test well, Wainwright, Alaska: Fairbanks, Alaska, Alaska Division of Geological and Geophysical Surveys Report of Investigations 2016-3-3, p. 37–58. https://doi.org/10.14509/29657

Helmold, K.P., Campaign, W.J., Morris, W.R., Hastings, D.S., and Moothart, S.R., 2006, Reservoir quality and petrophysical model of the Tarn deep-water slope-apron system, North Slope, Alaska: Pacific Section, American Association of Petroleum Geologists annual meeting, Anchorage, Alaska.

Helmold, K.P., LePain, D.L., and Harun, N.T., 2021, Qualitative assessment of composition and reservoir quality of Albian–Cenomanian Nanushuk Formation sandstones, measured outcrop sections, central North Slope, Alaska: Alaska Division of Geological & Geophysical Surveys Raw Data File 2021-13, 7 p. https://doi.org/10.14509/30746

Herriott, T.M., Wartes, M.A., Decker, P.L., Gillis, R.J., Shellenbaum, D.P., Willingham, A.L., and Mauel, D.J., 2018, Geologic map of the Umiat-Gubik area, central North Slope, Alaska: Alaska Division of Geological & Geophysical Surveys Report of Investigation 2018-6, 55 p.

Houseknecht, D.W., 2019, Petroleum systems framework of significant new oil discoveries in a giant Cretaceous (Aptian-Cenomanian) clinotherm in Arctic Alaska: American Association of

Petroleum Geologists Bulletin, v. 103, no. 3, p. 619–652.

Houseknecht, D.W., Bird, K.J., and Schenk, C.J., 2008, Seismic analysis of clinoform depositional sequences and shelf-margin trajectories in Lower Cretaceous (Albian) strata, Alaska North Slope: Basin Research, v. 21, no. 5, p. 644–654. https://doi.org/10.1111/j.1365-2117.2008.00392.x

Houseknecht, D.W., and Schenk, C.J., 2001, Depositional sequences and facies in the Torok Formation, National Petroleum Reserve–Alaska (NPRA), *in* Houseknecht, D.W., ed., NPRA Core Workshop: Petroleum Plays and Systems in the National Petroleum Reserve–Alaska, p. 179–199.

Huffman, A.C., Ahlbrandt, T.S., Pasternack, I., Stricker, G.D., and Fox, J.E., 1985, Depositional and sedimentologic factors affecting the reservoir potential of the Cretaceous Nanushuk Group, central North Slope, Alaska, *in* Huffman, A.C., ed., Geology of the Nanushuk Group and related rocks, North Slope, Alaska: U.S. Geological Survey Bulletin 1614, p. 61–74.

Ingersoll, R.V., Bullard, T.F., Ford, R.L., Grimm, J.P., Pickle, J.D., and Sares, S.W., 1984, The effect of grain size on detrital modes: A test of the Gazzi-Dickinson point-counting method: Journal of Sedimentary Petrology, v. 54, p. 103–116.

Johnsson, M.J., and Sokol, N.K., 2000, Stratigraphic variation in petrographic composition of Nanushuk Group sandstones at Slope Mountain, North Slope, Alaska, *in* Kelley, K.D., and Gough, L.P., eds., Geologic studies in Alaska by the U. S. Geological Survey, 1998: U.S. Geological Survey Professional Paper 1615, p. 83–100.

LePain, D.L., and Kirkham, R.A., 2001, Potential reservoir facies in the Nanushuk Formation (Albian-Cenomanian), central North Slope, Alaska: Examples from outcrop and core, *in* Houseknecht, D.W., ed., NPRA core workshop: Petroleum plays and systems in the National Petroleum Reserve in Alaska: SEPM Core Workshop 21, p. 19–36.

LePain, D.L., McCarthy, P.J., and Kirkham, R.A., 2009, Sedimentology and sequence stratigraphy of the middle Albian-Cenomanian Nanushuk Formation in outcrop, central North Slope, Alaska: Alaska Division of Geological & Geophysical Surveys Report of Investigation 2009-1 v. 2, 76 p., 1 sheet. http://doi.org/10.14509/19761

Lundegard, P.D., 1992, Sandstone porosity loss; a "big picture" view of the importance of compaction: Journal of Sedimentary Petrology, v. 62, no. 2, p. 250–260.

Molenaar, C.M., 1985, Subsurface correlations and depositional history of the Nanushuk Group and related strata, North Slope, Alaska, *in* Huffman, A.C., ed., Geology of the Nanushuk Group and related rocks, North Slope, Alaska: U.S. Geological Survey Bulletin 1614, p. 61–74.

Molenaar, C.M., Egbert, R.M., and Krystinik, L.F., 1988, Depositional facies, petrography, and reservoir potential of the Fortress Mountain Formation (Lower Cretaceous), central North Slope, Alaska *in* Gryc, George, ed., Geology and exploration of the National Petroleum Reserve in Alaska, 1974 to 1982: U.S. Geological Survey Professional Paper 1399, p. 257–280.

Moore, T.E., Wallace, W.K., Bird, K.J., Karl, S.M., Mull, C.G., and Dillon, J.T., 1994, Geology of northern Alaska, *in* Plafker, George, and Berg, H.C., eds., The Geology of Alaska: Geological Society of America, p. 49–138.

Mull, C.G., Houseknecht, D.W., and Bird, K.J., 2003, Revised Cretaceous and Tertiary stratigraphic nomenclature in the Coleville Basin, northern Alaska: U.S. Geological Survey Professional Paper 1673, 51 p.

Paxton, S.T., Szabo, J.O., Ajdukiewicz, J.M., and Klimentidis, R.E., 2002, Construction of an intergranular volume compaction curve for evaluating and predicting compaction and porosity loss in rigid-grain sandstone reservoirs: American Association of Petroleum Geologist Bulletin, v. 86, no. 12, p. 2,047–2,067.

Reifenstuhl, R.R., and Loveland, Andrea, 2004, Reservoir characterization study: porosity and permeability of 148 Tertiary to Mississippian age outcrop samples, east-central Brooks Range Foothills and North Slope, Alaska: Alaska Division of Geological & Geophysical Surveys Preliminary Interpretive Report 2004-5, 21 p. https://doi.org/10.14509/3312

Robinson, F.M., 1958, Test Well Grandstand Area Alaska: U.S. Geological Survey Professional Paper 305-E, p. 317–338.

Robinson, F.M., and Collins, F.R., 1959, Core Test, Sentinel Hill Area and Test Well Fish Creek Area, Alaska: U.S. Geological Survey Professional Paper 305-I, p. 485–520.

Scherer, M., 1987, Parameters influencing porosity in sandstones: A model for sandstone porosity prediction: American Association of Petroleum Geologist Bulletin, v. 71, no. 5, p. 485–491.

Shimer, G.T., McCarthy, P.J., and Hanks, C.L., 2014, Sedimentology, stratigraphy, and reservoir properties of an unconventional, shallow, frozen petroleum reservoir in the Cretaceous Nanushuk Formation at Umiat field, North Slope, Alaska: Association of Petroleum Geologist Bulletin, v. 98, no. 4, p. 631–661.

Smosna, Richard, 1989, Compaction law for Cretaceous sandstones of Alaska's North Slope: Journal of Sedimentary Petrology, v. 59, no. 4, p. 572–584.

Szabo, J.O., and Paxton, S.T., 1991, Intergranular volume (IGV) decline curves for evaluating and predicting compaction and porosity loss in sandstones [abs.]: Association of Petroleum Geologist Bulletin, v. 75, no. 3, p. 678.

Velleman, P.F., 1998, Learning data analysis with the student version of Data Desk 6.0: Ithaca, New York, Addison-Wesley, 362 p.

Wartes, M.A., 2008, Evaluation of stratigraphic continuity between the Fortress Mountain and Nanushuk Formations in the central Brooks Range foothills—Are they partly correlative?, *in* Wartes, M.A., and Decker, P.L., eds., Preliminary results of recent geologic field investigations in the Brooks Range Foothills and North Slope, Alaska: Alaska Division of Geological & Geophysical Surveys Preliminary Interpretive Report 2008-1C, p. 25–39. http://doi.org/10.14509/16087

Wilson, F.H., Hults, C.P., Mull, C.G., and Karl, S.M., 2015, Geologic Map of Alaska: U.S. Geological Survey Scientific Investigations Map 3340, pamphlet 197p., 2 sheets, scale 1:1,584,000. http://pubs.er.usgs.gov/publication/sim3340 (on DVD)